Supplementary Material (ESI) for Chemical Communications

Planar triazinium cations from VO^{2+}-assisted ring cyclizations: a remarkably efficient thiazole species for nuclear staining, PDT and anaerobic photocleavage of DNA

Puja Prasad,[a] Imran Khan,[b] Pijus K. Sasmal,[a] Debasis Koley,[a] Paturu Kondaiah,[b] and Akhil R. Chakravarty*[a]

[a] Department of Inorganic and Physical Chemistry, Indian Institute of Science and [b] Department of Molecular Reproduction, Development and Genetics, Indian Institute of Science, Bangalore 560012, India. E-mail: arc@ipc.iisc.ernet.in

Electronic Supplementary Information (ESI)

Experimental Section

Materials and measurements

All reagents and chemicals were procured from commercial sources (SD Fine Chemicals, India; Aldrich, USA) and used without further purifications. Solvents used were purified by standard procedures.[S1] Supercoiled (SC) pUC19 DNA (cesium chloride purified) was purchased from Bangalore Genie (India). Tris-(hydroxylmethyl)aminomethane-HCl (Tris-HCl) buffer solution was prepared using deionized and sonicated triple distilled water. Calf thymus (CT) DNA, agarose (molecular biology grade), catalase, superoxide dismutase (SOD), 2,2,6,6-tetramethyl-4-piperidone (TEMP), 1,4-diazabicyclo-[2.2.2]octan (DABCO), ethidium bromide (EB), bromophenol blue, were from Sigma (USA). 1-(2-pyridylazo)-2-naphthol (H-PAN) starting material was bought from SD Fine Chemical, India. The ligand 1-(2-thiazolylazo)-2-naphthol (H-TAN) was prepared by using literature procedure.[S2]

The elemental analysis was done using a Thermo Finnigan Flash EA 1112 CHNS analyzer. The infrared and electronic spectra were recorded on Perkin Elmer Lambda 35 and Perkin Elmer Spectrum one 55 spectrophotometers, respectively. Cyclic voltammetric measurements were made at 25 °C on a EG&G PAR Model 253 VersaStat potentiostat/galvanostat with electrochemical analysis software 270 using a three electrode set-up comprising of a glassy carbon working, platinum wire auxiliary and a saturated calomel reference (SCE) electrode. TBAP (0.1 M) was used as a supporting electrolyte in DMF. The electrochemical data were uncorrected for junction potentials. Electrospray ionization mass spectral measurements were done using Esquire 3000 plus ESI (Bruker Daltonics) and Q-TOF Mass Spectrometer. Fluorescence microscopic investigations were carried out on Zeiss, LSM510 apocromat.

Preparation of compound 1 and 2:

Method 1

Vanadyl sulfate (0.18 g, 1.0 mmol) was dissolved in 10 ml of MeOH and reacted with a aqueous solution of $Ca(ClO_4)_2 \cdot 4H_2O$ (0.31 g, 1.0 mmol). The mixture was stirred at an ambient temperature for 2 h. $CaSO_4$ precipitated out from the reaction was filtered out using celite and the blue coloured filtrate was collected. To this filtrate was added an equivalent amount of H-TAN (0.25, 1.0 mmol) for compound **1** and H-PAN (0.24, 1.0mmol) for compound **2**. The above solution was stirred for one day at an ambient temperature. The solution was filtered to obtain greenish brown precipitate. The compound was dissolved in acetonitrile and allowed for slow evaporation to get greenish brown colour crystals. The crystals thus obtained was washed with chloroform and dried by washing with diethyl ether [Yield: ~85% (**1**) and ~75% (**2**)].

Method 2

The azo H-TAN and H-PAN for compound **1** and **2** respectively, was dissolved in acetonitrile and to it equal volume of aqueous $HClO_4$ (0.01M) was added and stirred for 5 days. The orange solution turned into pale yellow colour. The above solution was evaporated and the crude product thus obtained was washed thoroughly with chloroform. Pure product was obtained by crystallizaion in acetonitile-toluene mixture. The solid obtained was washed with diethyl ether [Yield: ~65% (**1**) and ~63% (**2**)].

CAUTION! *The perchlorate salts could be potentially explosive. Therefore, only small quantities of the sample were handled to avoid any possible explosion*

Characterization data

Compound **1**: Anal. Calcd for $C_{13}H_8N_3O_4ClS$: C, 46.23; H, 2.39; N, 12.44. Found: C, 46.16; H, 2.37; N, 12.46. ESI-MS in CH_3CN: m/z 238.2 $[M]^+$, ^{1}H NMR (CD_3CN): δ 9.589 (d, J = 8.0 Hz, 1H), 9.226 (d, J = 4.4 Hz, 1H), 8.906 (d, J = 9.6 Hz, 1H), 8.779 (d, J = 4 Hz, 1H), 8.475 (d, J = 9.2 Hz, 1H), 8.317 (d, J = 8.0 Hz, 1H), 8.136 (dd, $J_1 = J_2$ =7.6 Hz, 1H), 8.050 (dd, $J_1 = J_2$ =7.6 Hz, 1H). ^{13}C NMR (CD_3CN): δ 160.672, 145.026, 141.711, 133.384, 132.974, 132.291, 130.612, 130.502, 128.938, 126.760, 126.449, 124.471, 113.489. UV-vis in 2% aq. DMF [λ_{max}/nm (ε/dm^3 mol^{-1} cm^{-1}]: 611sh (150), 440 (10300), 324sh (3990), 290 (8450), 242 (24760) and 208 (20950). IR (KBr phase, cm^{-1}): 3092s, 1573w, 1503w, 1383s (N=N), 1304w, 1220w, 1170w, 1083vs (ClO_4^-), 835w, 786m, 622s. (vs, very strong; s, strong; m, medium; w, weak). Λ_M = 74 S m^2 M^{-1} in DMF at 25 ºC.

Compound **2**: Anal. Calcd for $C_{15}H_{10}N_3O_4Cl$: C, 54.31; H, 3.04; N, 12.67. Found: C, 54.30; H, 3.07; N, 12.69. ESI-MS in CH_3CN: m/z 238.2 $[M]^+$,. ^{1}H NMR (CD_3CN): δ 10.001 (d, J = 6.8 Hz, 1H), 9.795 (d, J = 8.4 Hz, 1H), 9.350 (q, J_1 = 1.2 Hz, J_2 = 7.2 Hz, J_3 = 1.2 Hz, 1H), 9.029 (m, 2H), 8.790 (d, J = 9.2 Hz, 1H), 8.608 (dd, $J_1 = J_2$ = 6.8 Hz, 1H), 8.450 (d, J_1 =8 Hz, 1H), 8.264 (m, 1H), 8.17 (m, 1H). ^{13}C NMR (CD_3CN): 144.965, 143.352, 134.096, 132.756, 132.269, 131.276, 130.185, 129.763, 128.965, 126.872, 126.143, 124.712, 123.165, 122.395, 112.651. UV-vis in 2% aq. DMF [λ_{max}/nm (ε/dm^3 mol^{-1} cm^{-1})]: 568 sh (75), 437 (4170), 299 (7790), (8447), 240 sh(3938), 223 (10326) and 204 (11240). IR (KBr phase, cm^{-1}): 3737br, 1583w, 1347m (N=N), 1076vs (ClO_4^-), 827w, 785w, 618s (br, broad). Λ_M = 76 S m^2 M^{-1} in DMF at 25 ºC.

Solubility and stability

The compounds were soluble in H_2O, CH_3CN, DMF, DMSO; partially soluble in MeOH and EtOH and insoluble in hydrocarbon solvents. They were stable in both the solid and solution phases.

X-ray crystallographic procedures

The crystal structures of compounds **1** and **2** were obtained by single crystal X-ray diffraction technique. Crystals were obtained from slow evaporation of the acetonitrile solutions of the compounds. Crystal mounting was done on glass fibre with epoxy cement. All geometric and intensity data were collected at room temperature using an automated Bruker SMART APEX CCD diffractometer equipped with a fine focus 1.75 kW sealed tube Mo-K_α X-ray source (λ = 0.71073 Å) with increasing ω (width of 0.3° per frame) at a scan speed of 5 and 15 seconds per frame for compounds **1** and **2**, respectively. Intensity data, collected using ω-2θ scan mode, were corrected for Lorentz–polarization effects and for absorption.[S3] Structure was solved by the combination of Patterson and Fourier techniques and refined by full-matrix least-squares method using SHELX system of programs.[S4] All hydrogen atoms belonging to the complex were in their calculated positions and refined using a riding model. All non-hydrogen atoms were refined anisotropically. Perspective view of the molecule was obtained by ORTEP.[S5]

Confocal studies: Uptake and PDT effect

Uptake of fluorescent compounds **1** and **2** into the cell were visualized using a confocal scanning electron microscope (Zeiss, LSM510 apocromat). HeLa cells were grown on glass cover slips in each 12 well plates at a seeding density of 50,000 cells in 1.5 ml of culture medium

for 24 h. Later cells were treated with compounds for 4 h, 8 h and 12 h in dark. Cells were fixed and permeabilized with chilled methanol for 20 min at -20 °C. Later methanol was removed and was washed with 1XPBS. It was later incubated with Propidium iodide (10 mg/ml) to stain nucleus for 2 min and visualized under a confocal scanning electron microscope. To view the PDT effect we did the experiment putting one of the dishes in light for 45 min.

Flow cytometric analysis (FACS)

In order to confirm the confocal findings of uptake studies, Flow cytometric analysis was performed. $0.3x10^6$ HeLa cells were plated per well of a 6-well tissue culture plate in Dulbecco's Modified Eagle Medium (DMEM) containing 10% FBS. After 24 h of incubation at 37 °C in a CO_2 incubator, compound **1** and **2** (20 μM) were added to the cells with different incubation time point (1h, 2h and 4 h) in dark. After this incubation period, cells were trypsinized and collected into 1.5 ml centrifuge tubes. The cells were then washed once with chilled phosphate buffer saline of pH 7.4 and fixed by adding 800 μL of chilled 70% ethanol drop-wise with constant and gentle vortexing to prevent cell aggregation. The cell suspension was incubated at -20 °C for 6 h. The fixed cells were then washed two times with 1 ml of chilled PBS by centrifuging at 4000 rpm for 5 min at 4° C. The supernatant was discarded by gently inverting the tube and the cell pellet was suspended in 200 μL of PBS containing 10 μg ml^{-1} DNAse-free RNAse for 12 h at 37° C for digesting the cellular RNA. After RNAse digestion cells were washed twice with DPBS. Flow cytometric analysis was performed using FACS Calibur (Becton Dickinson (BD) cell analyzer) at FL2 channel (488 nm).

Cell cytotoxicity assay

The photocytotoxicity of the compounds **1** and **2** was studied using 3-(4,5-dimethylthiazol-2-yl)-2,5-diphenyltetrazolium bromide (MTT) assay which is based on the ability of mitochondrial dehydrogenases of viable cells to cleave the tetrazolium rings of MTT forming dark purple membrane impermeable crystals of formazan that could be quantified from spectral measurement in DMSO.[S6] Approximately, 8000 cells of human cervical cancer HeLa cells and MCF-7 cells were plated in 96 wells culture plate in Dulbecco's Modified Eagle Medium (DMEM) containing 10% FBS and after 24 h of incubation at 37 °C in CO_2 incubator, various concentrations of compound **1** and **2** dissolved in 0.005% DMSO were added to the cells and incubation was continued for 24 h in dark. The medium that was subsequently replaced with PBS was photo-irradiated with visible light (400-700 nm) for 1 h using a Luzchem Photoreactor (Model LZC-1, Ontario, Canada) fitted with Sylvania make 8 fluorescent white tubes with a fluence rate of 2.4 mW cm^{-2} to provide a total dose of 10 J cm^{-2}. After photoexposure, PBS was removed and replaced with DMEM-FBS and incubation was continued for further 20 h in dark. After the incubation period, 25 μL of 5 mg mL^{-1} of MTT was added to each well and incubated for an additional 3 h. The culture medium was finally discarded and 200 μL of DMSO was added to dissolve the formazan crystals and its absorbance at 595 nm was measured using a BIORAD ELISA plate reader. Cytotoxicity of compound **1** and **2** was measured as the percentage ratio of the absorbance of the treated cells to the untreated controls. The IC_{50} values were determined by nonlinear regression analysis (GraphPad Prism).

DNA fragmentation analysis by agarose gel electrophoresis

DNA fragmentation analysis was conducted to confirm the apoptotic mechanism induced by compound **1** for cell death. Briefly $0.3x10^6$ cells were taken in each 60mm dish. It was grown for 24 h and later treated with **1** (20 μg/ml) for 6 h in dark. Light was exposed to one of the dish for 1 h and again the cells were left to grow for 4 h along with its dark control. After 4 h, cells were trypsinized, washed with DPBS and re-suspended in 0.4 ml of lysis buffer (10 mM Tris-HCl; pH, 8.0, 20 mM EDTA, 0.2% triton-X 100) with an incubation of 20 min on ice. Lysed cells were centrifuged for 20 min at 13000 rpm and their supernatant (which has soluble chromosomal DNAs including both high molecular weight DNA and nucleosomal DNA fragments) was collected. Phenol chloroform was performed to remove the protein present. Later supernatant was precipitated with 1/10 volume of 3M sodium acetate (pH, 5.8) and 2 volume of ethanol at -20 °C for overnight. DNA pellet was washed with 70% alcohol and re-suspended in TE containing RNAse (1X Tris-EDTA with 100 μg/ml RNAse). DNA samples were placed into the well of 1.5% agarose gel. The agarose gels were run at 70 volts for approximately 2 h before photographed under UV light.

DNA binding methods

The experiments were carried out in Tris-HCl buffer (5 mM, pH 7.2) using the compound solution of 100 μM in DMF (0.1%) The calf thymus (CT) DNA (ca. 350 μM NP) in the buffer medium gave a ratio of UV absorbance at 260 and 280 nm of ca. 1.9:1 suggesting the DNA apparently free from protein. The concentration of DNA was estimated from its absorption intensity at 260 nm with a known molar absorption coefficient value of 6600 $dm^3\ mol^{-1}\ cm^{-1}$.[S7] Absorption titration experiments were performed by varying the concentration of the CT DNA while keeping the complex concentration as constant. Due correction was made for the

absorbance of DNA itself. The spectra were recorded after equilibration for 5 min. The intrinsic equilibrium binding constant (K_b) and the binding site size (s) of the complexes to CT DNA were obtained by McGhee-von Hippel (MvH) method using the expression of Bard and co-workers by monitoring the change of the absorption intensity of the spectral bands with increasing concentration of CT DNA by regression analysis using equation (1)

$$(\varepsilon_a-\varepsilon_f)/(\varepsilon_b-\varepsilon_f) = (b-(b^2-2K_b^2C_t[\mathrm{DNA}]_t/s)^{1/2})/2K_bC_t, \text{-------(1)}$$

$$b = 1 + K_bC_t + K_b[\mathrm{DNA}]_t/2s,$$

where ε_a is the extinction coefficient observed for the charge transfer absorption band at a given DNA concentration, ε_f is the extinction coefficient of the complex free in solution, ε_b is the extinction coefficient of the complex when fully bound to DNA, K_b is the equilibrium binding constant, C_t is the total metal complex concentration, $[\mathrm{DNA}]_t$ is the DNA concentration in nucleotides and s is the binding site size in base pairs.[S8,S9] The non-linear least-squares analysis was done using Origin Lab, version 6.1.

DNA melting experiments were carried out by monitoring the absorption intensity of CT DNA (140 μM) at 260 nm at various temperatures, both in the absence and presence of the compound **1** and **2** (14 μM). Measurements were carried out using a Cary 300 bio UV-vis spectrometer with a Cary temperature controller with increasing the temperature of the solution by 0.5 °C per min.

DNA cleavage experiments

The cleavage of supercoiled pUC19 DNA (30 μM, 0.2 μg, 2686 base-pair) was studied by agarose gel electrophoresis using compound **1** and **2** in 50 mM tris(hydroxymethyl)methane-HCl (Tris-HCl) buffer (pH 7.2) containing 50 mM NaCl. For photo-induced DNA cleavage

studies in visible light at different wavelength of 458 nm, 488 nm, 514 nm, 647 nm using a Spectra Physics Water-Cooled Mixed-Gas Ion Laser Stabilite® 2018-RM (Continuous-wave (CW) beam diameter at $1/e^2$ 1.8 mm ± 10% and beam divergence with full angle 0.7 mrad ± 10%). The laser beam power at the sample position (5 cm from the aperture with a solution path length of 5 mm) was 60 mW, measured using Spectra Physics CW Laser Power Meter (Model 407A). The experiments were carried out both in aerobic and anaerobic conditions. After light exposure, each sample was incubated for 30 min at 37 °C and analyzed for the photo-cleaved products using gel electrophoresis. The mechanistic studies were carried out using different additives (KI, 1 mM; DMSO, 6 μl, catalase, 6 units; SOD, 6 units; TEMP, 1 mM; DABCO, 1 mM) prior to the addition of the complex. For the D_2O experiment, this solvent was used for dilution of the sample to 20 μL. The samples after incubation in a dark chamber were added to the loading buffer containing 0.25% bromophenol blue, 0.25% xylene cyanol, 30% glycerol (3 μL) and the solution was finally loaded on 1% agarose gel containing 1.0 μg/mL ethidium bromide. Electrophoresis was carried out in a dark chamber for 2.0 h at 60 V in TAE (Tris-acetate EDTA) buffer. Bands were visualized by UV light and photographed. The extent of DNA cleavage was measured from the intensities of the bands using UVITEC Gel Documentation System. Due corrections were made for the low level of nicked circular (NC) form present in the original supercoiled (SC) DNA sample and for the low affinity of EB binding to SC compared to NC and linear forms of DNA.[S10] The concentrations of the complexes and additives corresponded to that in the 20 μL final volume of the sample using Tris buffer. The observed error in measuring the band intensities was ~5%.

Computational Details

All calculations were performed with the Gaussian03 and Gaussian09 suites of program.[S11] The DFT calculations employed the B3LYP functional[S12] using the standard 6-311+G**[S13] basis sets and the solvent (water, dielectric constant ε = 80) effect were incorporated using the polarized continuum model.[S14] Geometries of the ground and excited states were fully optimized, normally without symmetry constraints. The electronic singlet to singlet (S0-Sn) transitions in water were computed using the linear response time-dependent density functional theory (TD-DFT).[S15]

References:

(S1) D. D. Perrin, W. L. F. Armarego and D. R. Perrin, *Purification of Laboratory Chemicals*; Pergamon Press: Oxford, 1980.

(S2) B. S. Jenesen, *Acta Chem. Scand*., 1960, **14**, 927-932.

(S3) N. Walker and D. Stuart, *Acta Crystallogr., Sect. A*, 1983, **A39**, 158-166.

(S4) G. M. Sheldrick, *SHELX-97, Programs for Crystal Structure Solution and Refinement*; University of Göttingen, Göttingen, Germany, 1997.

(S5) C. K. Johnson, *ORTEP, Report ORNL-5138*; Oak Ridge National Laboratory: Oak Ridge, TN, 1976.

(S6) T. Mosmann, *J. Immunol. Methods*, 1983, **65**, 55-63.

(S7) M. E. Reichman, S. A. Rice, C. A. Thomas and P. Doty, *J. Am. Chem. Soc.*, 1954, **76**, 3047-3053.

(S8) J. D. McGhee and P. H. von Hippel, *J. Mol. Biol.*, 1974, **86**, 469-489.

(S9) M. T. Carter, M. Rodriguez and A. J. Bard, *J. Am. Chem. Soc.*, 1989, **111**, 8901-8911.

(S10) J. Bernadou, G. Pratviel, F. Bennis, M. Girardet and B. Meunier, *Biochemistry* 1989, **28**, 7268-7275.

(S11) Gaussian 09, Revision A.1, M. J. Frisch, G. W. Trucks, H. B. Schlegel, G. E. Scuseria, M. A. Robb, J. R. Cheeseman, G. Scalmani, V. Barone, B. Mennucci, G. A. Petersson, H. Nakatsuji, M. Caricato, X. Li, H. P. Hratchian, A. F. Izmaylov, J. Bloino, G. Zheng, J. L. Sonnenberg, M. Hada, M. Ehara, K. Toyota, R. Fukuda, J. Hasegawa, M. Ishida, T. Nakajima, Y. Honda, O. Kitao, H. Nakai, T. Vreven, J. A. Montgomery, Jr., J. E. Peralta, F. Ogliaro, M. Bearpark, J. J. Heyd, E. Brothers, K. N. Kudin, V. N. Staroverov, R. Kobayashi, J. Normand, K. Raghavachari, A. Rendell, J. C. Burant, S. S. Iyengar, J. Tomasi, M. Cossi, N. Rega, J. M. Millam, M. Klene, J. E. Knox, J. B. Cross, V. Bakken, C. Adamo, J. Jaramillo, R. Gomperts, R. E. Stratmann, O. Yazyev, A. J. Austin, R. Cammi, C. Pomelli, J. W. Ochterski, R. L. Martin, K. Morokuma, V. G. Zakrzewski, G. A. Voth, P. Salvador, J. J. Dannenberg, S. Dapprich, A. D. Daniels, Ö. Farkas, J. B. Foresman, J. V. Ortiz, J. Cioslowski, and D. J. Fox, Gaussian, Inc., Wallingford CT, 2009.

(S12) (a) A. D. Becke, *Phys. Rev. A*, 1988, **38**, 3098-3100. (b) A. D. Becke, *J. Chem. Phys.*, 1993, **98**, 5648-5652. (c) C. Lee, W. Yang, R. G. Parr, *Phys. Rev. B*, 1988, **37**, 785-789.

(S13) W. J. Hehre, L. Radom, P. v. R. Schleyer, J. A. Pople, *Ab Initio Molecular Orbital Theory*, Wiley, New York, 1986, pp 65-68.

(S14) J. Tomasi, M. Persico, *Chem Rev.*, 1994, **94**, 2027-2094.

(S15) (a) M. E. Casida, C. Jamorski, K. C. Casida, D. R. Salahub, *J. Chem. Phys.*, 1998, **108**, 4439-4449. (b) R. E. Stratmann, G. E. Scuseria, M. J. Frisch, *J. Chem. Phys.*, 1998, **109**, 8218-8224.

Table S1. Selected TDDFT singlet transitions depicted in Figure S23 are shown for both **1** and **2**. These TDDFT excitations are calculated from the PCM optimized ground state geometries of **1** and **2**

	Energy (eV)	Wavelength (nm)	Oscillator strength	Major contributions
I	2.749	451	0.2747	HOMO→LUMO (96%)
II	3.842	323	0.1739	HOMO-3→LUMO (91%)
				HOMO→LUMO+2 (5%)
III	4.474	277	0.2783	HOMO-1→LUMO+1 (67%)
				HOMO→LUMO+2 (25%)
IV	5.121	242	0.4886	HOMO-5→LUMO (33%)
				HOMO→LUMO+2 (35%)
I	2.800	443	0.2330	HOMO→LUMO (96%)
II	3.568	347	0.0768	HOMO→LUMO+1 (83%)
				HOMO-1→LUMO (12%)
III	4.196	295	0.6783	HOMO-1→LUMO+1 (67%)
				HOMO-3→LUMO (19%)
IV	5.429	228	0.4176	HOMO→LUMO+3 (38%)
				HOMO-4→LUMO+1 (15%)

Table S2. B3LYP/6-311+G**/PCM optimized geometries of **1** and **2**.

No.	Cartesian coordinates			
1 (S_0)	S	3.94257	-0.77690	0.00000
	N	0.16100	-1.70961	-0.00022
	N	1.46008	-1.84418	-0.00026
	N	1.72914	0.53092	-0.00009
	C	-3.85856	1.00762	0.00024
	H	-4.30792	1.99377	0.00031
	C	-4.64609	-0.12466	0.00025
	H	-5.72567	-0.03541	0.00034
	C	-4.04997	-1.40010	0.00016
	H	-4.67679	-2.28382	0.00018
	C	-2.67481	-1.53900	0.00005
	H	-2.22046	-2.52022	-0.00002
	C	-1.85194	-0.39690	0.00002
	C	-2.44964	0.89555	0.00013
	C	-1.61859	2.05405	0.00011
	H	-2.09236	3.02876	0.00017
	C	-0.24958	1.98215	0.00005
	H	0.34096	2.88647	0.00003
	C	0.35708	0.71316	-0.00003
	C	-0.40847	-0.48234	-0.00009
	C	2.21686	-0.74816	-0.00019
	C	3.96499	0.95442	-0.00016
	H	4.90268	1.48696	-0.00024
	C	2.72965	1.49885	0.00000
	H	2.48122	2.54592	-0.00003
1 (S_1)	S	3.96429	-0.79013	-0.00024
	N	0.13386	-1.73936	-0.00010
	N	1.47524	-1.84263	-0.00017
	N	1.74877	0.53778	-0.00008
	C	-3.88279	0.99947	0.00022
	H	-4.34268	1.98073	0.00028
	C	-4.67173	-0.14179	0.00021
	H	-5.75026	-0.05421	0.00027
	C	-4.06379	-1.39657	0.00013
	H	-4.66627	-2.29605	0.00013
	C	-2.65934	-1.51138	0.00006
	H	-2.19499	-2.48761	0.00000
	C	-1.83998	-0.36529	0.00006
	C	-2.44706	0.91595	0.00014
	C	-1.64844	2.07827	0.00015
	H	-2.11202	3.05585	0.00020

	C	-0.26312	1.97250	0.00007
	H	0.33476	2.87367	0.00007
	C	0.34803	0.70639	-0.00001
	C	-0.40408	-0.47962	-0.00002
	C	2.21621	-0.76505	-0.00016
	C	3.99198	0.95193	-0.00018
	H	4.92837	1.48535	-0.00021
	C	2.74990	1.48932	-0.00009
	H	2.51051	2.53977	-0.00003
2 (S_0)	N	0.11856	-1.79086	-0.00022
	N	1.38752	-1.98948	-0.00015
	N	1.82294	0.37651	-0.00005
	C	-3.77236	1.10739	-0.00003
	H	-4.17940	2.11168	-0.00006
	C	-4.60528	0.00968	0.00006
	H	-5.68031	0.14321	0.00008
	C	-4.06243	-1.29133	0.00012
	H	-4.72658	-2.14741	0.00021
	C	-2.69608	-1.48882	0.00008
	H	-2.28346	-2.48810	0.00012
	C	-1.82419	-0.38026	-0.00001
	C	-2.36861	0.93527	-0.00004
	C	-1.48418	2.04952	-0.00002
	H	-1.90760	3.04714	-0.00006
	C	-0.11972	1.91003	0.00006
	H	0.49478	2.79652	0.00028
	C	0.43696	0.61518	0.00000
	C	-0.38981	-0.52496	-0.00006
	C	2.25710	-0.93708	-0.00003
	C	3.63131	-1.21969	0.00012
	H	3.91621	-2.26250	0.00012
	C	4.54938	-0.19782	0.00020
	H	5.61050	-0.40858	0.00041
	C	4.08740	1.13011	0.00001
	H	4.77633	1.96335	-0.00006
	C	2.74599	1.39468	-0.00011
	H	2.36354	2.40003	-0.00029
2 (S_1)	N	0.08463	-1.81432	0.00005
	N	1.40169	-1.98692	0.00012
	N	1.84004	0.38100	-0.00000
	C	-3.79046	1.09932	0.00003
	H	-4.21074	2.09805	0.00004
	C	-4.63089	-0.01122	0.00001
	H	-5.70426	0.12555	0.00000
	C	-4.08136	-1.28958	-0.00001
	H	-4.72203	-2.16200	-0.00002

	C	-2.68350	-1.46241	-0.00000
	H	-2.25798	-2.45601	-0.00001
	C	-1.81419	-0.34828	0.00002
	C	-2.36440	0.95545	0.00003
	C	-1.50975	2.07623	0.00005
	H	-1.92377	3.07588	0.00008
	C	-0.13057	1.90240	0.00005
	H	0.49192	2.78493	0.00009
	C	0.42822	0.61432	0.00002
	C	-0.38856	-0.52664	0.00002
	C	2.25138	-0.95784	0.00010
	C	3.64551	-1.22577	0.00015
	H	3.93825	-2.26665	0.00025
	C	4.55962	-0.20592	0.00007
	H	5.62032	-0.42194	0.00012
	C	4.10692	1.13366	-0.00007
	H	4.79744	1.96470	-0.00016
	C	2.76223	1.38966	-0.00011
	H	2.38280	2.39775	-0.00022

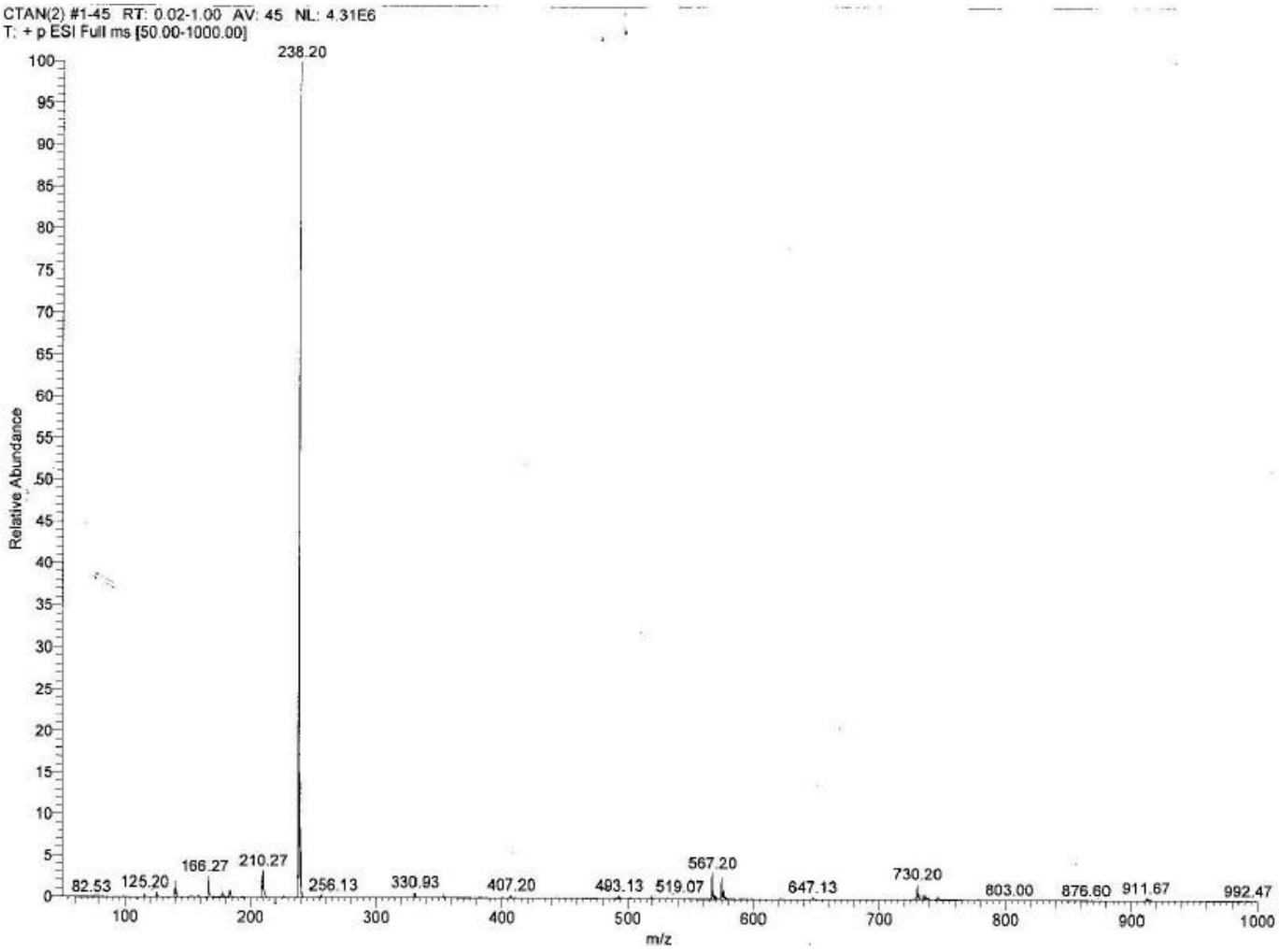

Fig. S1. The ESI-MS spectrum of the compound **1** showing the molecular ion peak at 238.20 (m/z) in CH_3CN.

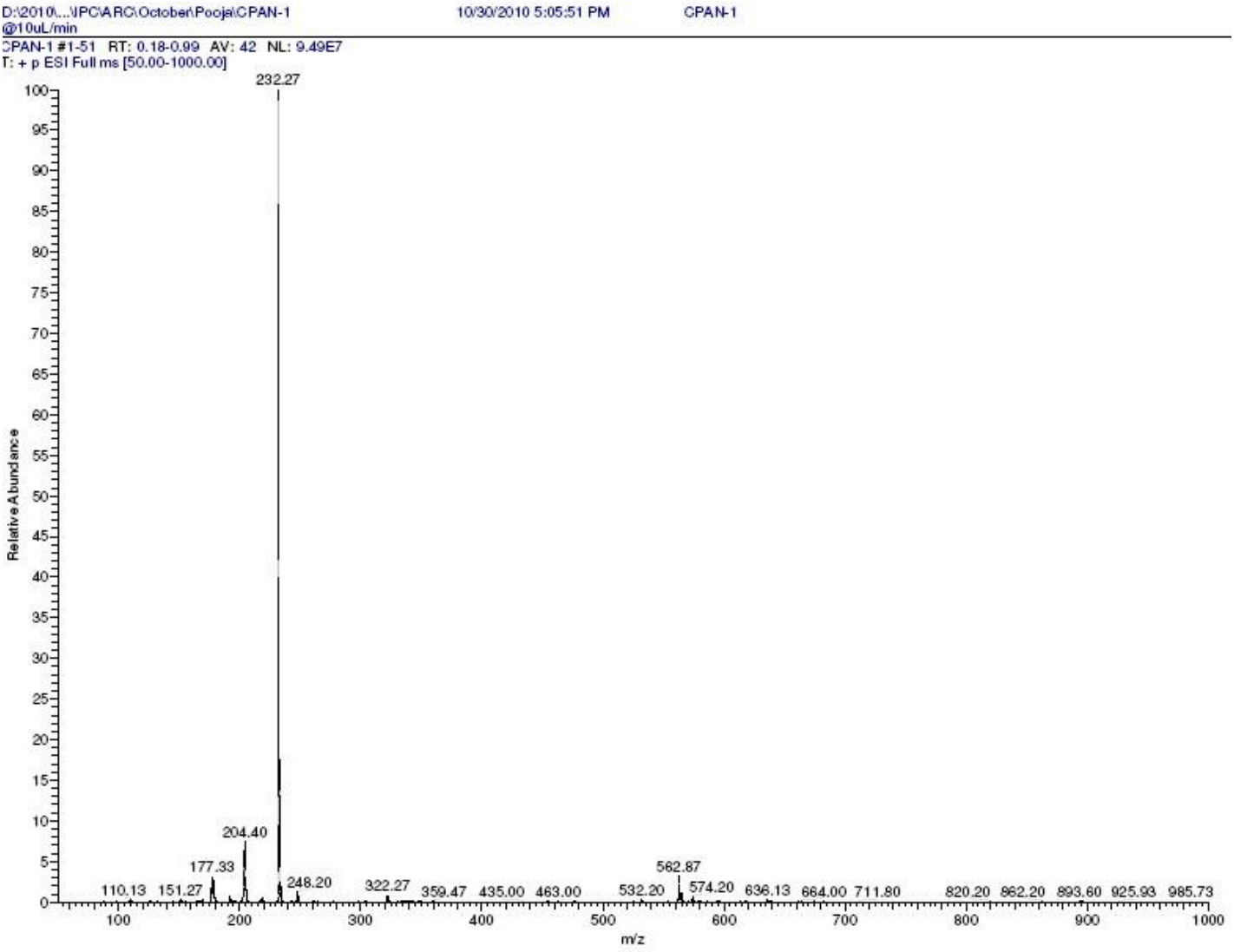

Fig. S2. The ESI-MS spectrum of the compound **2** showing the molecular ion peak at 232.27 (m/z) in CH_3CN.

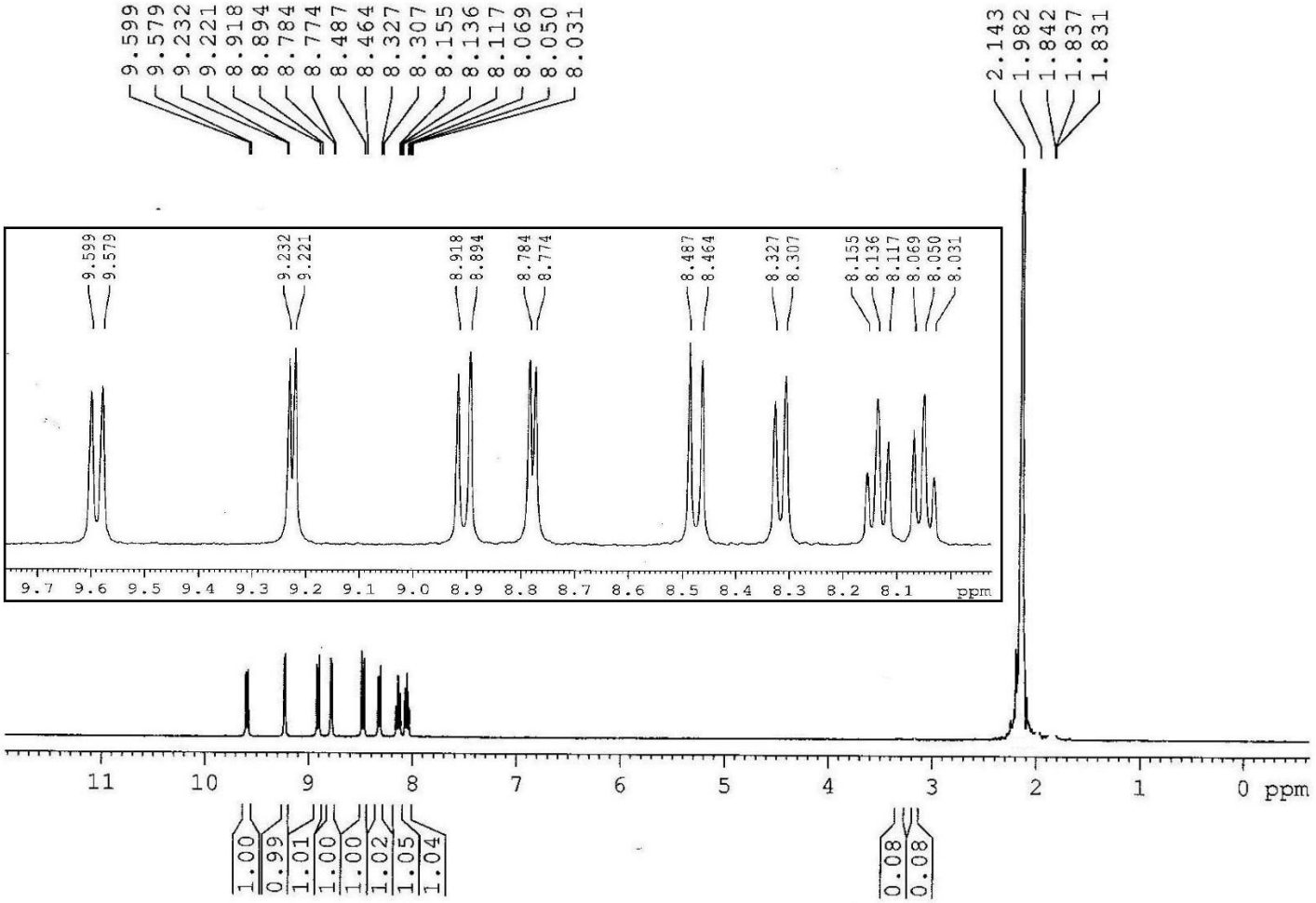

Fig. S3. ^{1}H NMR of **1** in CD_3CN.

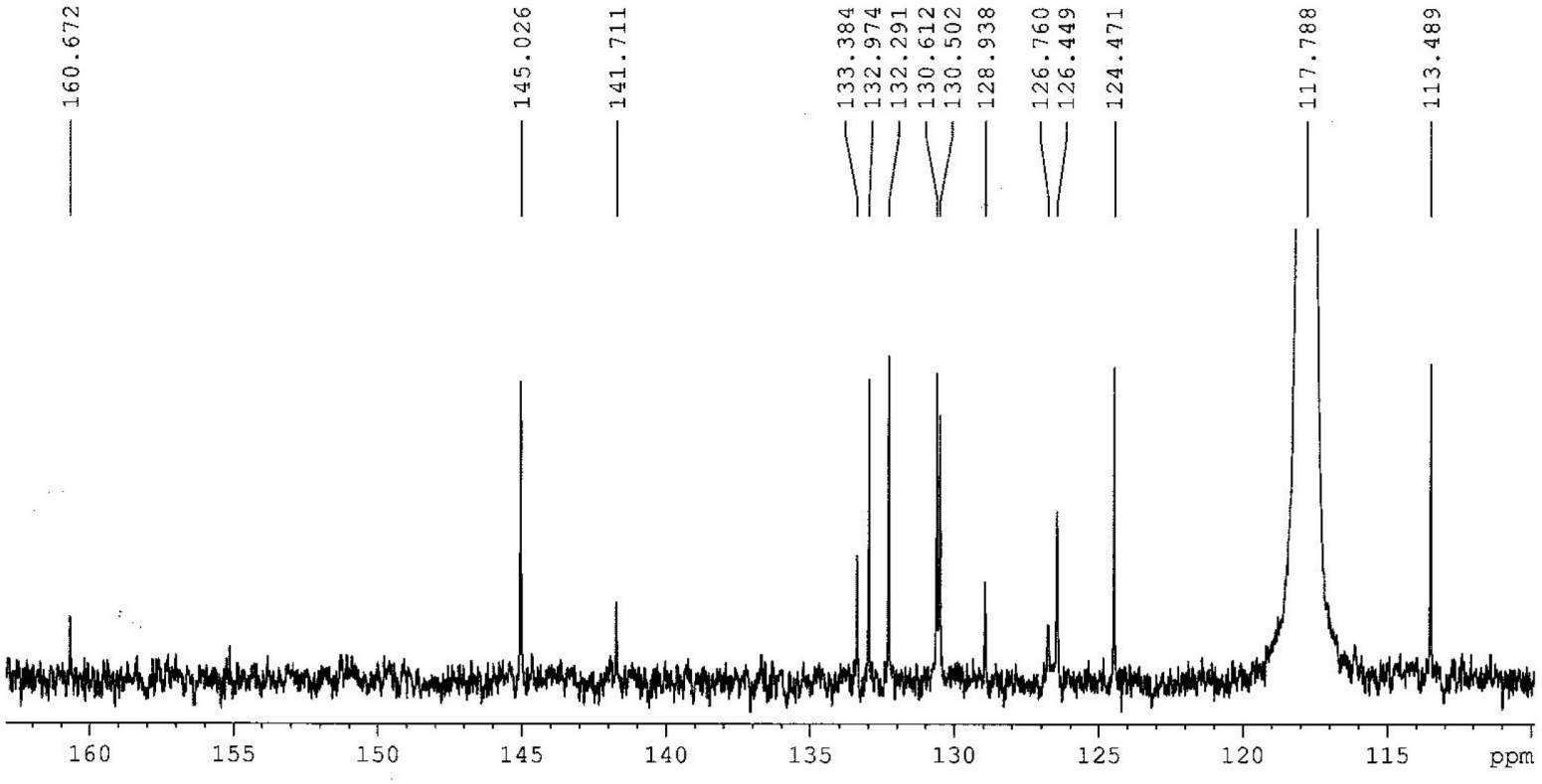

Fig. S4. ^{13}C NMR of **1** in CD_3CN.

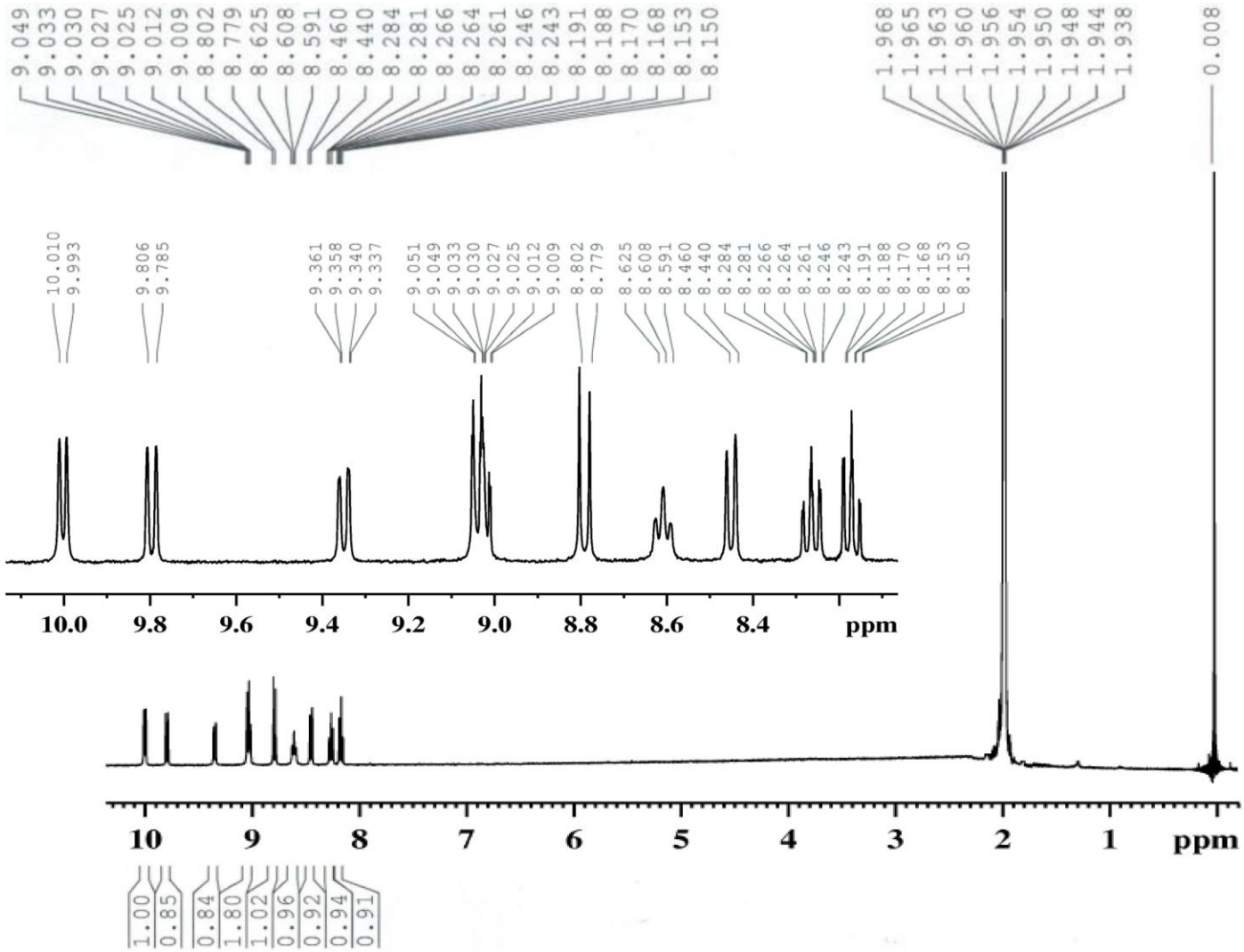

Fig. S5. ^{1}H NMR spectrum of **2** in CD_3CN.

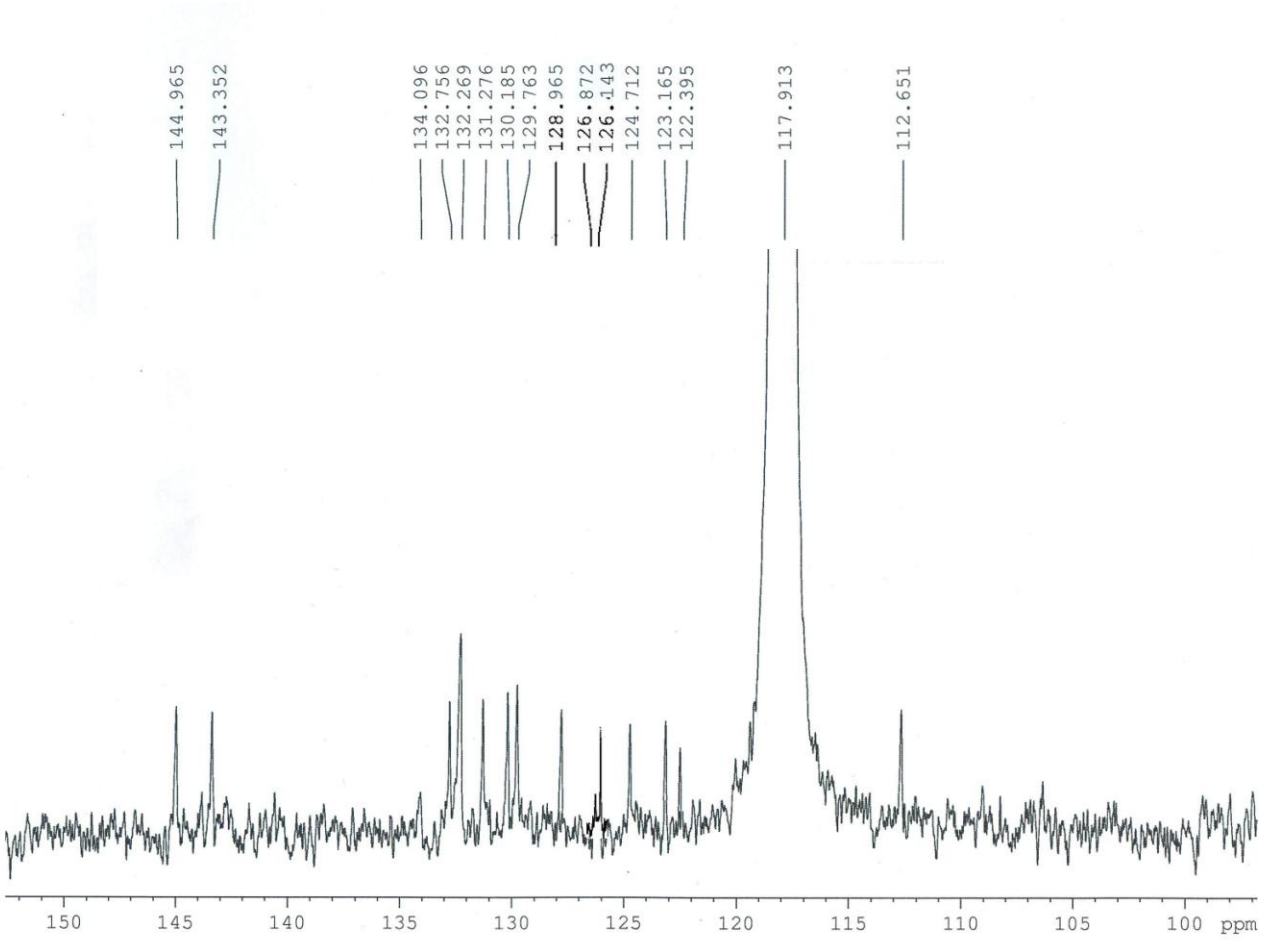

Fig. S6. ^{13}C NMR spectrum of **2** in CD_3CN.

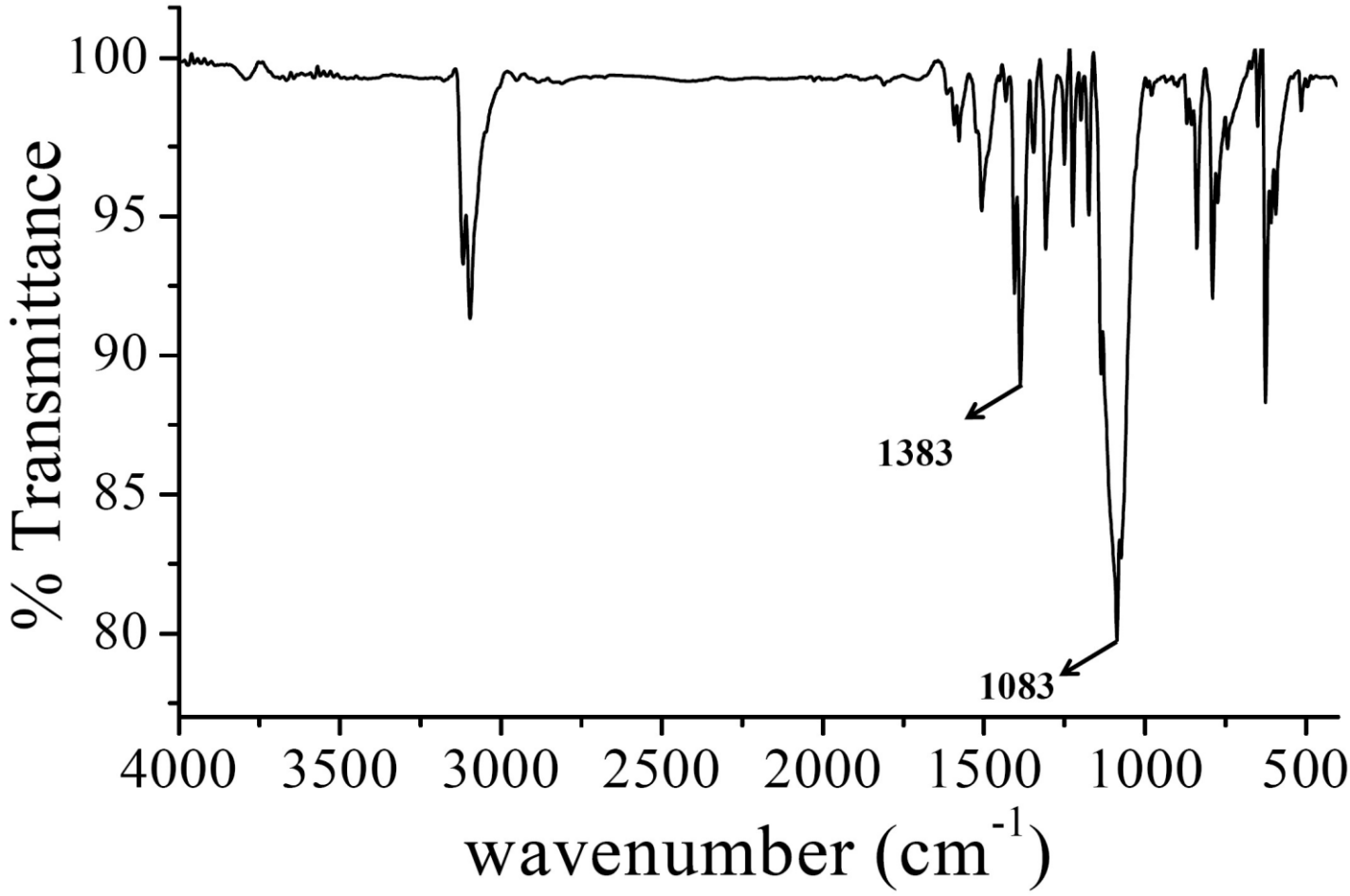

Fig. S7. IR spectrum of **1** in KBr phase showing characteristic peaks of N=N at 1383 cm^{-1} and ClO_4^- at 1083 cm^{-1}.

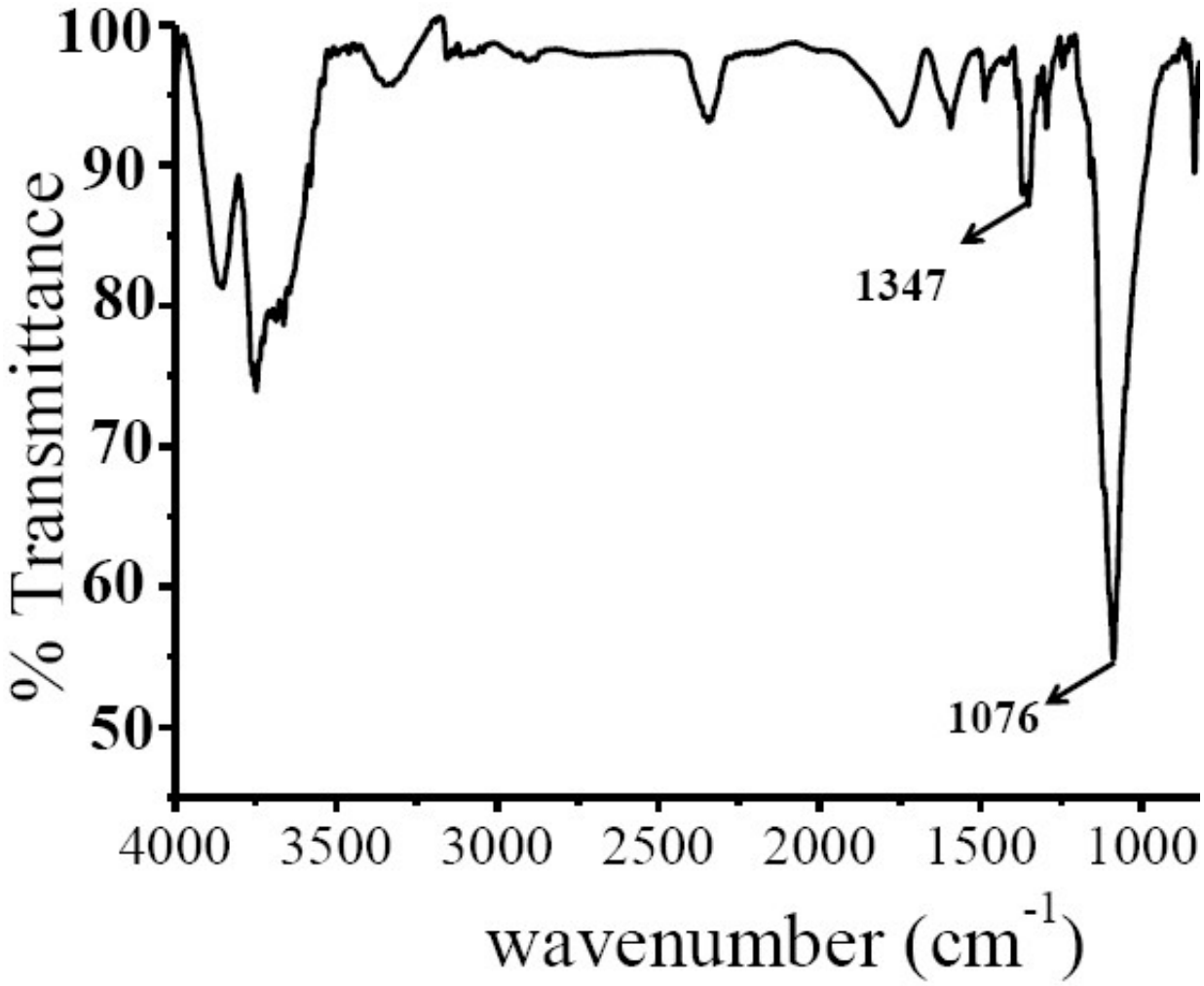

Fig. S8. IR spectrum of **2** in KBr phase showing characteristic peaks of N=N at 1347 cm^{-1} and ClO_4^- at 1076 cm^{-1}.

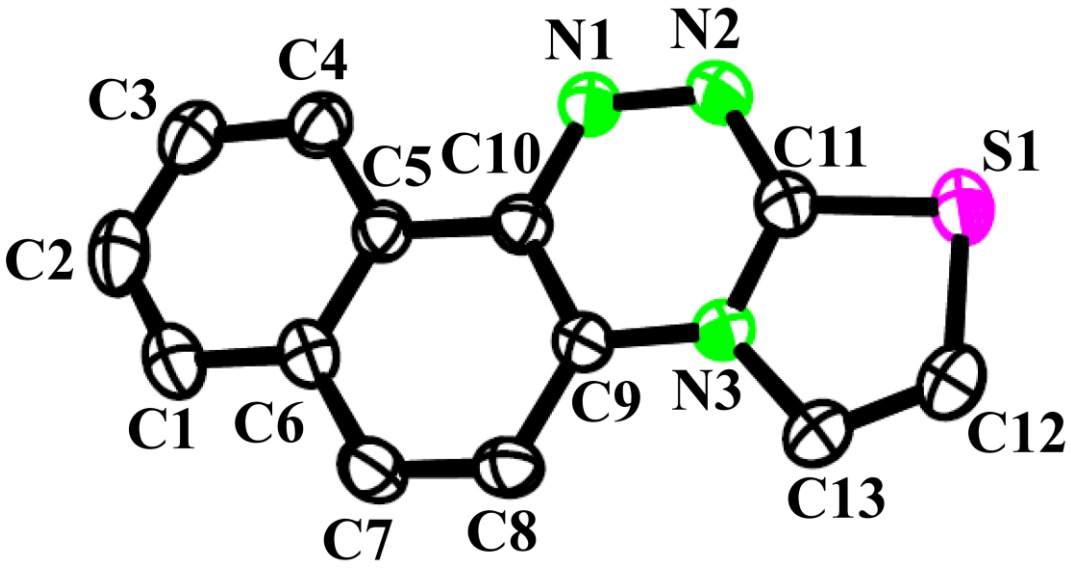

Fig. S9. An ORTEP view of the cationic compound **1** showing 50% probability thermal ellipsoids. The hydrogen atoms are not shown for clarity.

Selected Bond Distances (Å) and Angles (deg.) for **1** with e.s.d.s in the parenthesis			
S(1)-C(11)	1.705(2)	C(11)-S(1)-C(12)	90.01(12)
S(1)-C(12)	1.704(3)	S(1)-C(11)-N(2)	123.75(19)
N(1)-N(2)	1.309(3)	S(1)-C(11)-N(3)	112.22(17)
N(1)-C(10)	1.361(3)	S(1)-C(12)-C(13)	113.62(19)
N(2)-C(11)	1.347(3)	N(1)-N(2)-C(11)	118.7(2)
N(3)-C(9)	1.380(3)	N(1)-C(10)-C(9)	122.8(2)
N(3)-C(11)	1.363(3)	N(2)-N(1)-C(10)	120.1(2)
N(3)-C(13)	1.392(3)	N(2)-C(11)-N(3)	124.0(2)
C(9)-C(10)	1.401(3)	N(3)-C(9)-C(10)	115.62(19)
C(12)-C(13)	1.346(4)	N(3)-C(13)-C(12)	111.5(2)
		C(9)-N(3)-C(11)	118.59(19)
		C(11)-N(3)-C(13)	112.6(2)

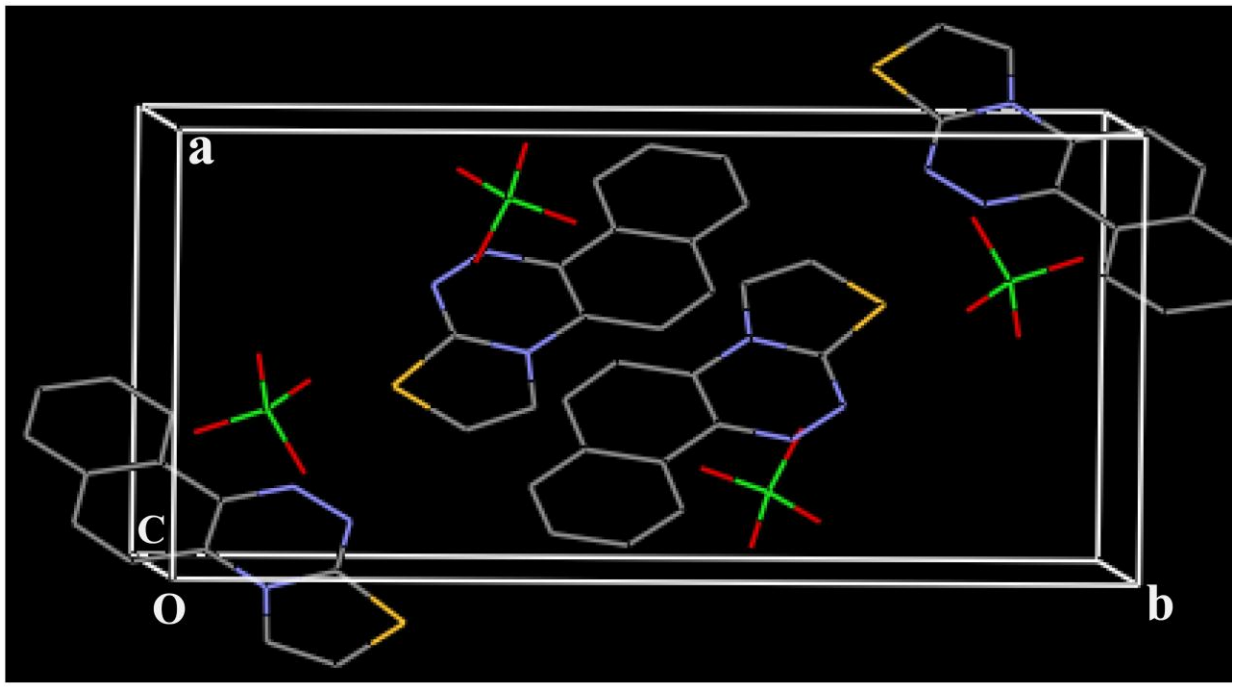

Fig. S10. Unit cell packing diagram of **1**.

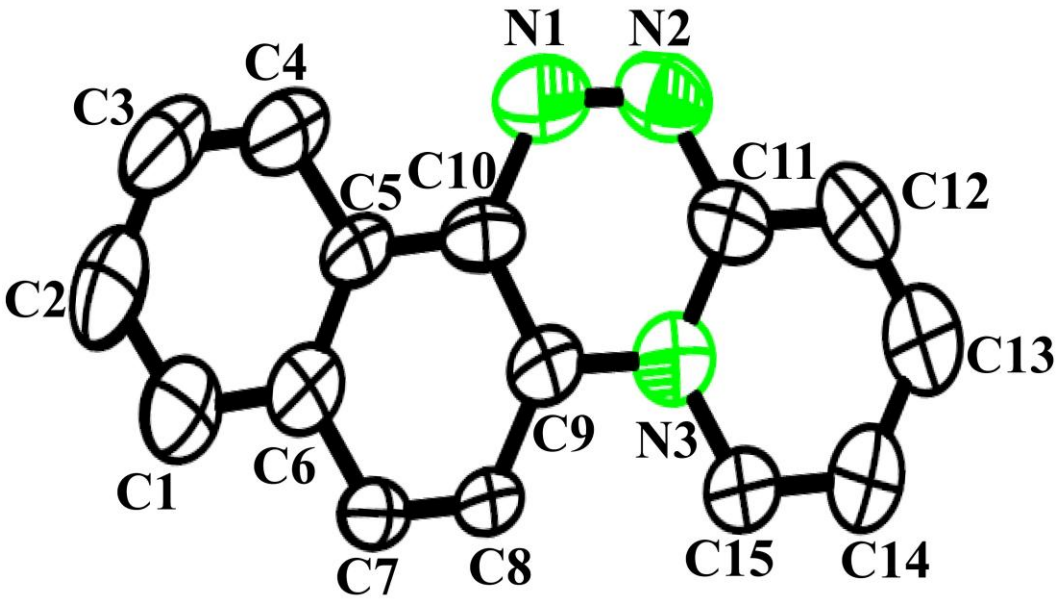

Fig.S11. An ORTEP view of the cationic compound **2** showing 50% probability thermal ellipsoids. The hydrogen atoms are not shown for clarity.

Selected Bond Distances (Å) and Angles (deg.) for **2** with e.s.d.s in the parenthesis			
N(1)-N(2)	1.372(7)	N(1)-N(2)-C(11)	122.8(4)
N(1)-C(10)	1.413(7)	N(1)-C(10)-C(9)	121.3(5)
N(2)-C(11)	1.408(7)	N(2)-N(1)-C(10)	117.7(4)
N(3)-C(9)	1.439(6)	N(2)-C(11)-N(3)	120.1(5)
N(3)-C(11)	1.388(6)	N(2)-C(11)-C(12)	121.1(4)
N(3)-C(15)	1.429(6)	N(3)-C(9)-C(10)	119.5(4)
C(9)-C(10)	1.405(6)	N(3)-C(11)-C(12)	118.7(4)
C(11)-C(12)	1.434(7)	N(3)-C(15)-C(14)	119.5(4)
C(12)-C(13)	1.363(8)	C(9)-N(3)-C(11)	118.5(4)
C(13)-C(14)	1.402(8)	C(11)-N(3)-C(15)	120.2(4)
C(14)-C(15)	1.383(6)	C(11)-C(12)-C(13)	120.4(5)
		C(12)-C(13)-C(14)	120.8(5)
		C(13)-C(14)-C(15)	120.2(5)

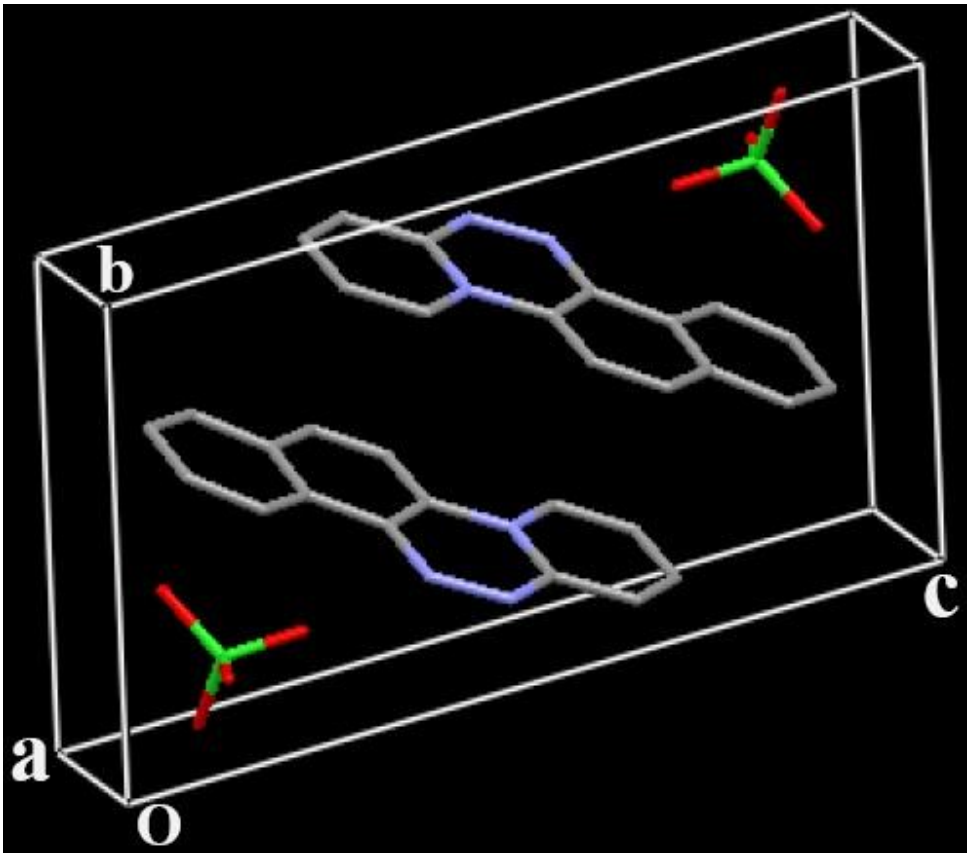

Fig. S12. Unit cell packing diagram of **2**.

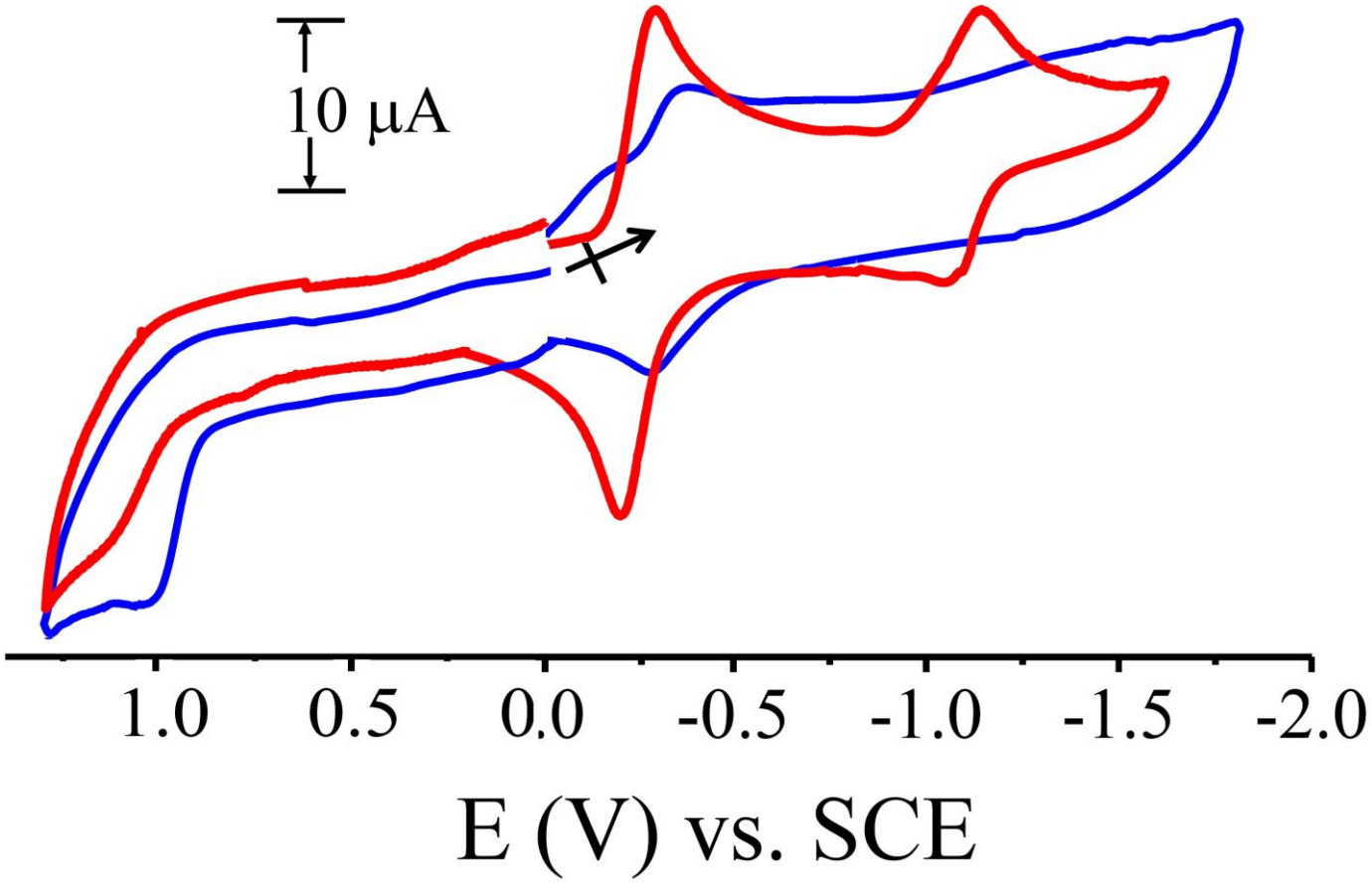

Fig. S13. Cyclic voltammograms of the compounds **1** (—) and **2** (—) in DMF buffer at a scan speed of 50 mV s^{-1} and 0.1 M TBAP as a supporting electrolyte.

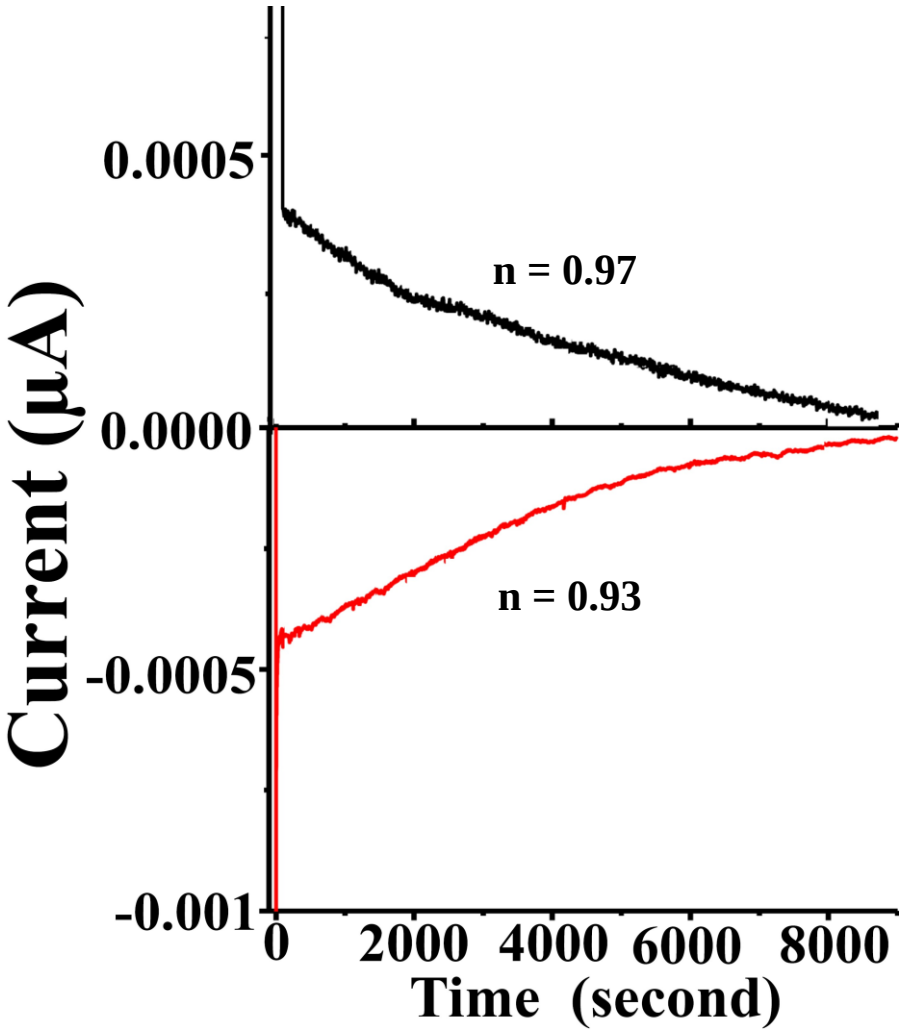

Fig. S14. Chronoamperometry at constant potential of 0.65 V for Ferrocene (─) as standard and –0.5 V for **1** (─) respectively, in DMF and 0.1 M TBAP showing one electron transfer.

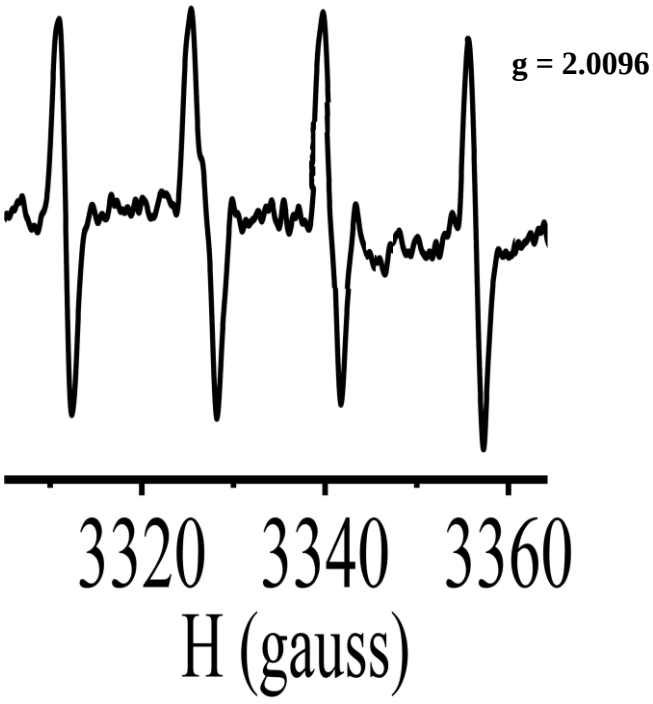

Fig. S15. EPR spectrum of **1** (0.01 M) with 5,5-dimethyl-1-pyrroline N-oxide (DMPO, 0.05 M) in DMF-Tris-HCl buffer (1:1 v/v) after electrolysis of compound **1** at constant potential of –0.5 V. The experimental conditions and operating frequency are T = 298 K, ν = 9.3775 GHz, modulation amplitude = 2.0 G at 100 kHz, and receiver gain = 1 x 10^{-4}.

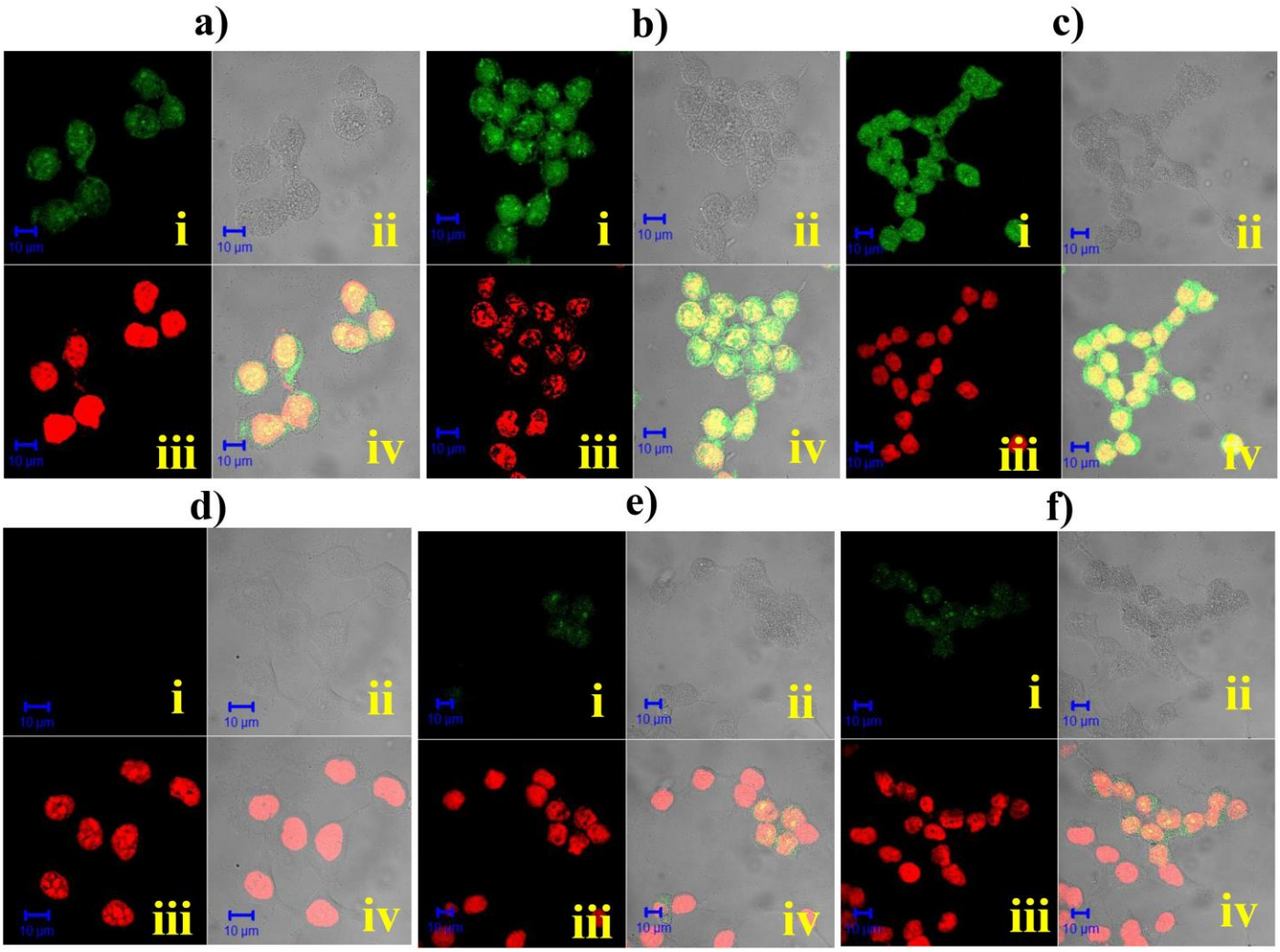

Fig. S16. Panels a,b,c and d, e, f are representative images of the HeLa cells treated with **1** and **2** at 4, 8 and 12 h, respectively, with 20 µM concentration. a,b,c,d,e,f-i:**1** and **2** florescence, a,b,c,d,e,f-ii: Bright field image, a,b,c,d,e,f-iii: PI staining, a,b,c,d,e,f-iv: merged . The uptake of compound **1** in the nucleus increases (yellow color) with time compared to compound **2** (marginal uptake) in dark. Scale Bar in blue corresponds to 10 µm.

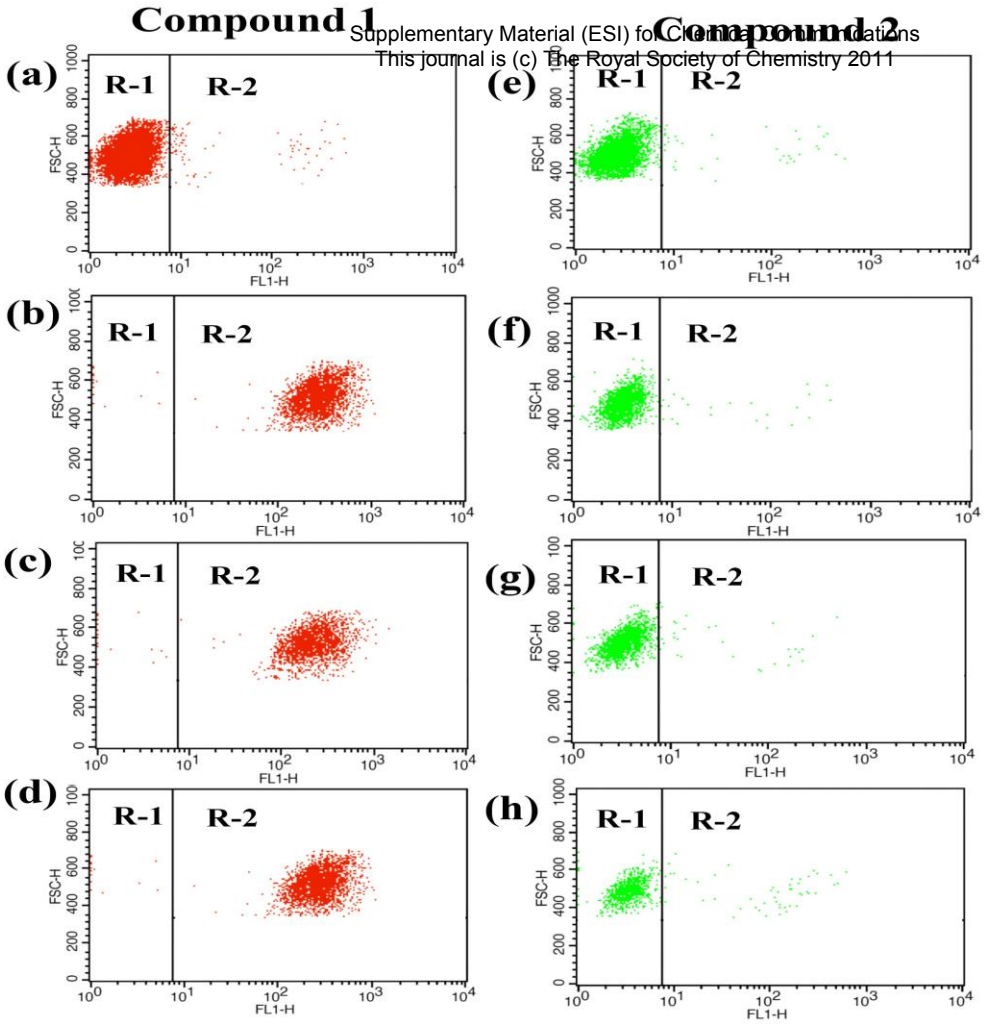

Fig. S17. Flow cytometric analysis (FACS) done for compound **1** (20µM): Panel (b-d) and compound **2** (20µM): Panel (f-h) at different incubation time of 1h, 2h and 4h in HeLa cells. Panel a and e indicates control (only cells) when no compounds added. Region R-1 indicates auto-florescence of cells and region R-2 indicates increase in florescence intensity of the cells due to uptake of compound.

	Panel No.	Incubation time	R-1(% Total)	R-2 (% Total)
control	a	4h	98.99	1.01
Compound **1**	b	1h	1.19	98.81
	c	2h	1.03	98.97
	d	4h	0.61	99.39
control	e	4h	99.16	0.84
Compound **2**	f	1h	98.05	1.95
	g	2h	94.18	5.82
	h	4h	88.00	12.00

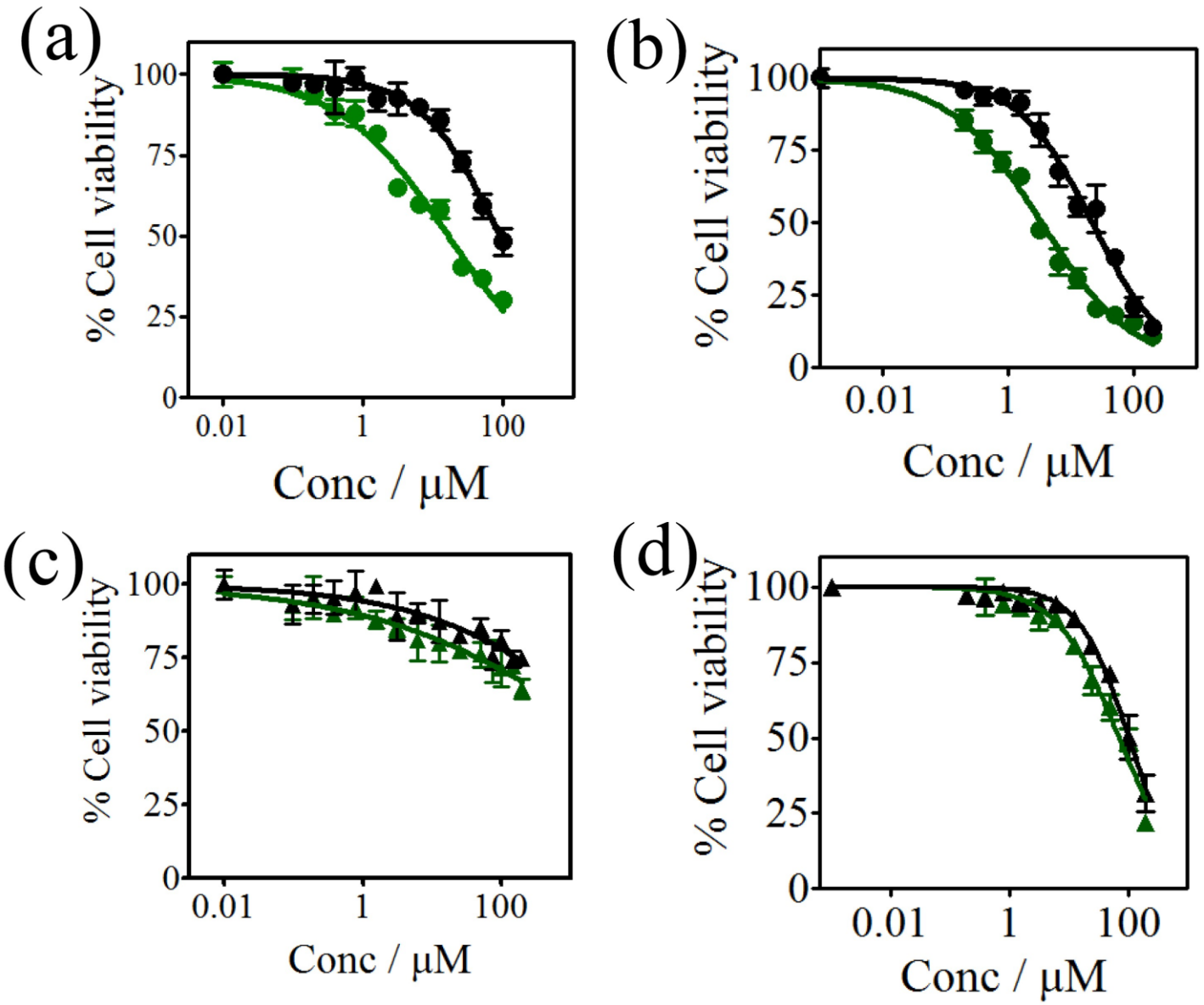

Fig. S18. Photocytotoxicity of compound **1** in (a) and (b) and compound **2** in (c) and (d) in cancer cells on 24 h incubation in dark followed upon photo-irradiation in visible light (400 to 700 nm) for 1 h as determined by MTT assay. Panels (a) and (c) are in HeLa cells and Panels (b) and (d) are in MCF-7 cells. The photo-exposed and dark-treated cells are shown in green and black color symbol, respectively.

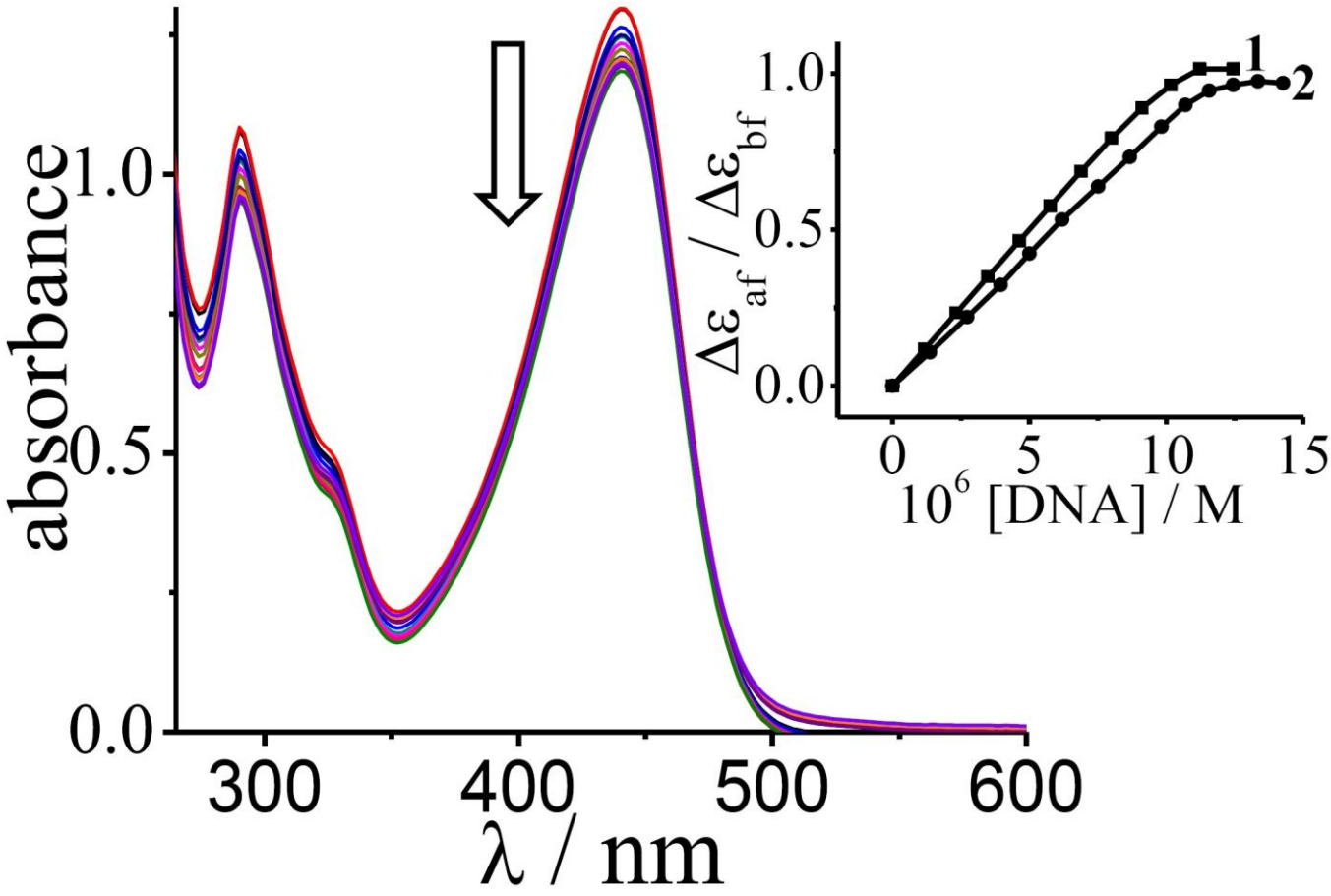

Fig. S19. Absorption spectral traces of **1** (100 µM) in 5 mM Tris-HCl buffer (pH 7.2) on increasing the concentration of CT DNA. The inset shows the least-squares fit of $\Delta\varepsilon_{af}/\Delta\varepsilon_{bf}$ vs. [DNA] for **1** (■) and **2** (●) using the MvH equation.

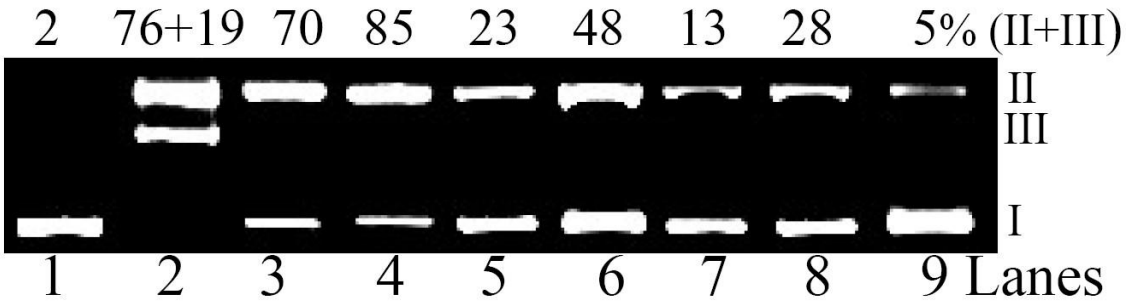

Fig. S20. Cleavage of SC pUC19 DNA (0.2 μg, 30 μM) by compound **1** and **2** (20 μM) in 50 mM Tris-HCl/NaCl buffer (pH, 7.2) containing 0.1% DMF in visible light of different wavelength for an exposure time of 2 h. Detailed reaction conditions are given below in a tabular form.

Lane No	λ/nm	Reaction conditions
1	458	DNA control
2	458	DNA + **1**
3	458	DNA + **2**
4	488	DNA + **1**
5	488	DNA + **2**
6	514	DNA + **1**
7	514	DNA + **2**
8	647	DNA + **1**
9	647	DNA + **2**

Fig. S21. Cleavage of SC pUC19 DNA (0.2 μg, 30 μM) by compound **1** and **2** (20 μM) in argon medium in 50 mM Tris-HCl/NaCl buffer (pH, 7.2) containing 0.1% DMF in visible light of different wavelength for an exposure time of 2 h. Detailed reaction conditions are given below in a tabular form.

Lane No	λ/nm	Reaction conditions
1	458	DNA control
2	458	DNA + **1**
3	458	DNA + **2**
4	488	DNA + **1**
5	488	DNA + **2**
6	514	DNA + **1**
7	514	DNA + **2**
8	647	DNA + **1**
9	647	DNA + **2**

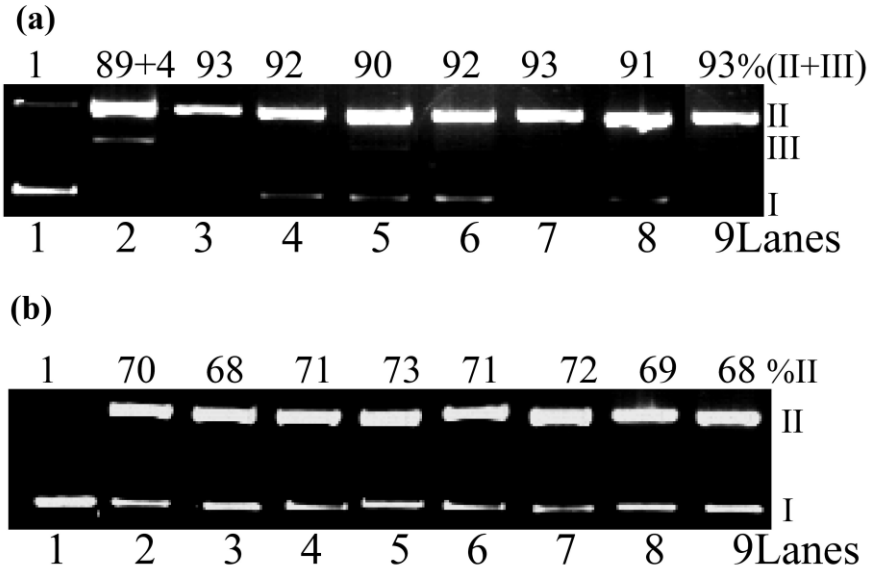

Fig. S22. Gel electrophoresis diagram displaying the photocleavage of SC pUC19 DNA (0.2 μg, 30 μM) at 458 nm by **1** (20 μM) in (a) and **2** (20 μM) in (b) in the presence of different additives for 1 h exposure time in 50 mM Tris-HCl / NaCl buffer (pH, 7.2). Detail conditions are given below in a tabular form.

Lane No.	Reaction condition
1	DNA
2	DNA + Compound
3	DNA + Compound + D_2O
4	DNA + Compound + TEMP (1 mM)
5	DNA + Compound + DABCO (1 mM)
6	DNA + Compound + KI (1 mM)
7	DNA + Compound + DMSO (6 μL)
8	DNA + Compound + Catalase (6 units)
9	DNA + Compound + SOD (6 units)

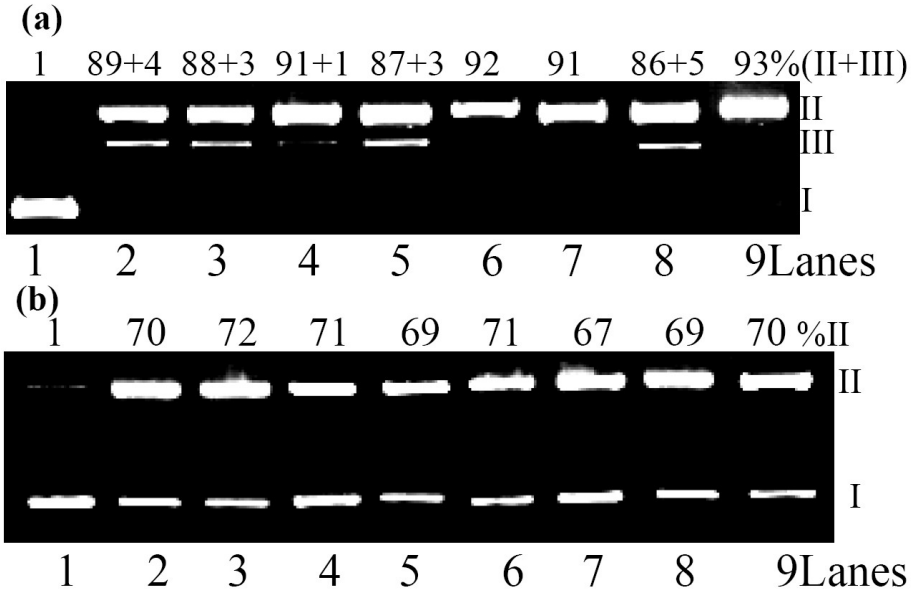

Fig. S23. Gel electrophoresis diagram displaying the photocleavage of SC pUC19 DNA (0.2 µg, 30 µM) at 458 nm by **1** (20 µM) in (a) and **2** (20 µM) in (b) in argon medium in the presence of different additives for 1 h exposure time in 50 mM Tris-HCl / NaCl buffer (pH, 7.2). Detail conditions are given below in a tabular form.

Lane No.	Reaction condition
1	DNA
2	DNA + Compound
3	DNA + Compound + D_2O
4	DNA + Compound + TEMP (1 mM)
5	DNA + Compound + DABCO (1 mM)
6	DNA + Compound + KI (1 mM)
7	DNA + Compound + DMSO (6 μL)
8	DNA + Compound + Catalase (6 units)
9	DNA + Compound + SOD (6 units)

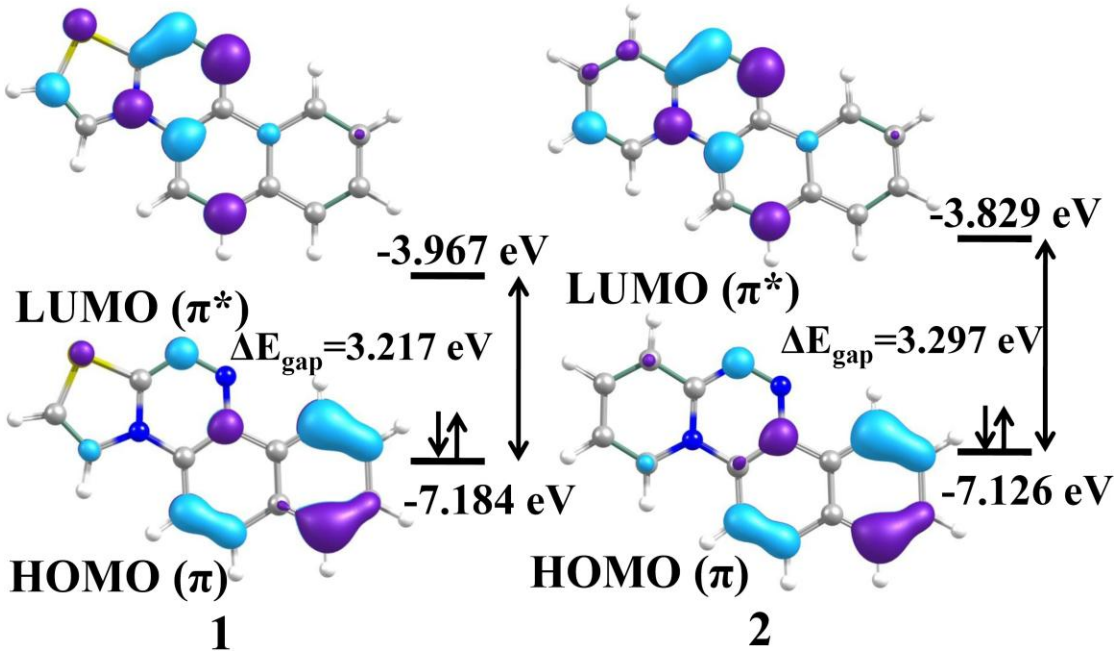

Fig. S24. The HOMO and LUMO of the compounds and the energy levels associated with them (ΔE_{gap} = 3.217 eV in **1** vs. 3.297 eV in **2**).

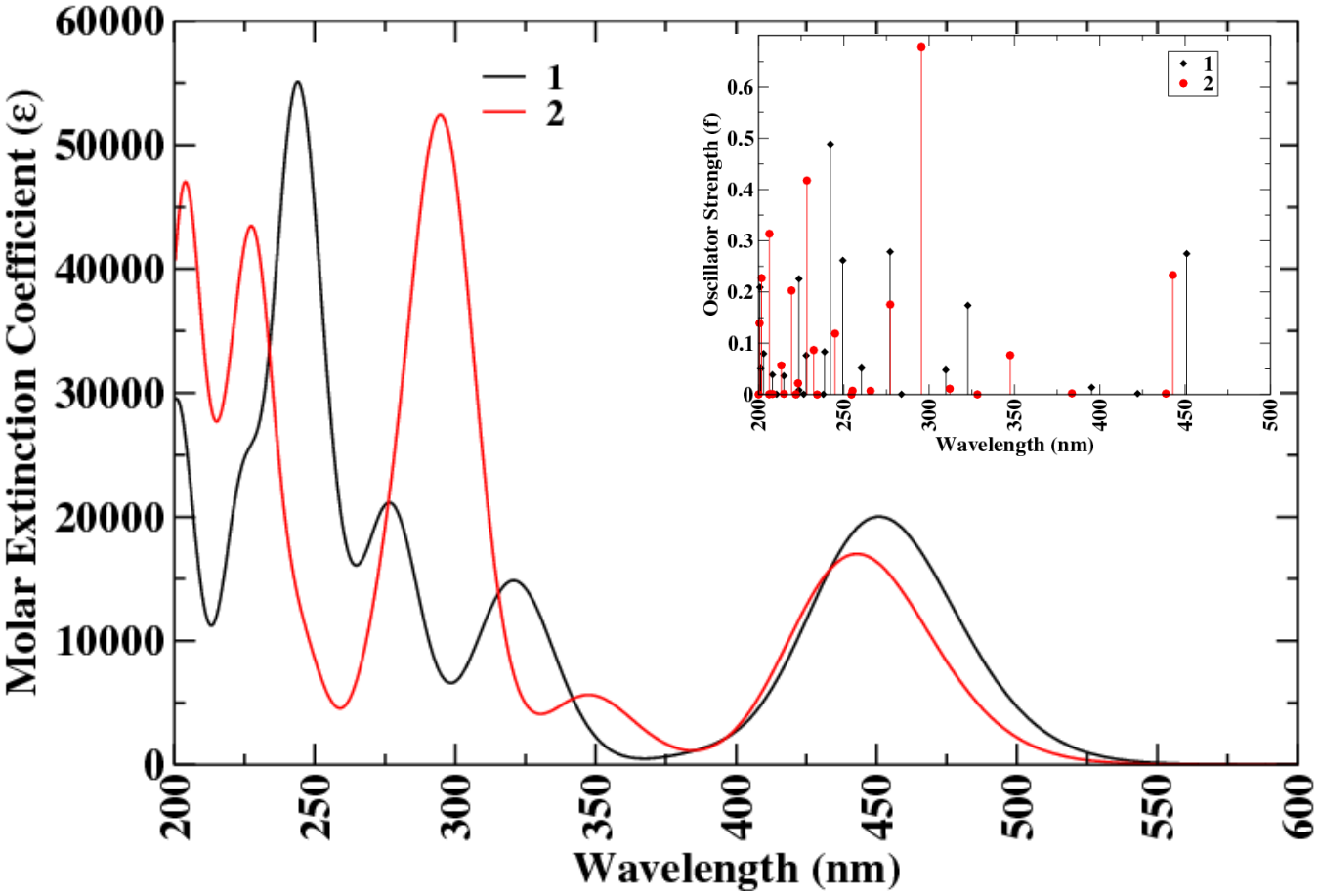

Fig. S25. Simulated UV-Visible spectra for **1** and **2** in aqueous solution. Inset: The oscillator strength for singlet-singlet transitions.